Glaciers of the Olympic Mountains, Washington - the past and future 100 years

Andrew G. Fountain[1], Christina Gray[1], Bryce Glenn[1], Brian Menounos[2], Justin Pflug[3], and Jon Riedel[4]

[1]Portland State University
[2]University of Northern British Columbia
[3]University of Washington
[4]United States National Park Service

November 26, 2022

Abstract

In 2015, the Olympic Mountains contain 255 glaciers and perennial snowfields totaling 25.34 ± 0.27 km^2, half of the area in 1900, and about 0.75 ± 0.19 km^3 of ice. Since 1980, glaciers shrank at a rate of -0.59 km^2 yr^{-1} during which 35 glaciers and 16 perennial snowfields disappeared. Area changes of Blue Glacier, the largest glacier in the study region, was a good proxy for glacier change of the entire region. A simple mass balance model of the glacier, based on monthly air temperature and precipitation, correlates with glacier area change. The mass balance is highly sensitive to changes in air temperature rather than precipitation, typical of maritime glaciers. In addition to increasing summer melt, warmer winter temperatures changed the phase of precipitation from snow to rain, reducing snow accumulation. Changes in glacier mass balance are highly correlated with the Pacific North American index, a proxy for atmospheric circulation patterns and controls air temperatures along the Pacific Coast of North America. Regime shifts of sea surface temperatures in the North Pacific, reflected in the Pacific Decadal Oscillation (PDO), trigger shifts in the trend of glacier mass balance. Negative ('cool') phases of the PDO are associated with glacier stability or slight mass gain whereas positive ('warm') phases are associated with mass loss and glacier retreat. Over the past century the overall retreat is due to warming air temperatures, almost +1°C in winter and +0.3°C in summer. The glaciers in the Olympic Mountains are expected to largely disappear by 2070.

Glaciers of the Olympic Mountains, Washington – the past and future 100 years

Andrew G. Fountain[1], Christina Gray[1], Bryce Glenn[1], Brian Menounos[2], Justin Pflug[2] Jon L. Riedel[3]

[1]Department of Geology, Portland State University, Portland, Oregon, USA

[2]Geography Program, University of Northern British Columbia, 3333 University Way, Prince George, British Columbia Canada

[3]Department of Civil and Environmental Engineering, University of Washington, Seattle, Washington, USA

[4]US National Park Service, North Cascades National Park, 810 State Route 20, Sedro-Woolley, Washington USA

Key Points:

- The glaciers of the Olympus Peninsula are shrinking rapidly, losing half of its ice-covered area since 1900
- Warming air temperatures are causing glacier loss; warming winter temperatures change the phase of the precipitation from snow to rain.
- Modeling suggests the glaciers will largely disappear by 2070

Corresponding author: Andrew G. Fountain, andrew@pdx.edu

Abstract

In 2015, the Olympic Mountains contain 255 glaciers and perennial snowfields totaling 25.34 ± 0.27 km^2, half of the area in 1900, and about 0.75 ± 0.19 km^3 of ice. Since 1980, glaciers shrank at a rate of -0.59 km^2 yr^{-1} during which 35 glaciers and 16 perennial snowfields disappeared. Area changes of Blue Glacier, the largest glacier in the study region, was a good proxy for glacier change of the entire region. A simple mass balance model of the glacier, based on monthly air temperature and precipitation, correlates with glacier area change. The mass balance is highly sensitive to changes in air temperature rather than precipitation, typical of maritime glaciers. In addition to increasing summer melt, warmer winter temperatures changed the phase of precipitation from snow to rain, reducing snow accumulation. Changes in glacier mass balance are highly correlated with the Pacific North American index, a proxy for atmospheric circulation patterns and controls air temperatures along the Pacific Coast of North America. Regime shifts of sea surface temperatures in the North Pacific, reflected in the Pacific Decadal Oscillation (PDO), trigger shifts in the trend of glacier mass balance. Negative ('cool') phases of the PDO are associated with glacier stability or slight mass gain whereas positive ('warm') phases are associated with mass loss and glacier retreat. Over the past century the overall retreat is due to warming air temperatures, almost +1°C in winter and +0.3°C in summer. The glaciers in the Olympic Mountains are expected to largely disappear by 2070.

1. Introduction

The Olympic Mountains are the western-most alpine terrain in the Pacific Northwest US, isolated on the Olympic Peninsula of Washington State. These mountains are first to intercept moisture-laden storms originating over the Pacific Ocean with the highest peak (Mt. Olympus) 56 km inland. Although the mountains only reach to 2432 m above sea level (asl), glaciers mantle the highest mountains due to the heavy winter snowfall and cool summers.

Precipitation varies from 3000 mm yr^{-1} on the west side of the range to only 500 mm yr^{-1} on the east (Rasmussen et al., 2001).

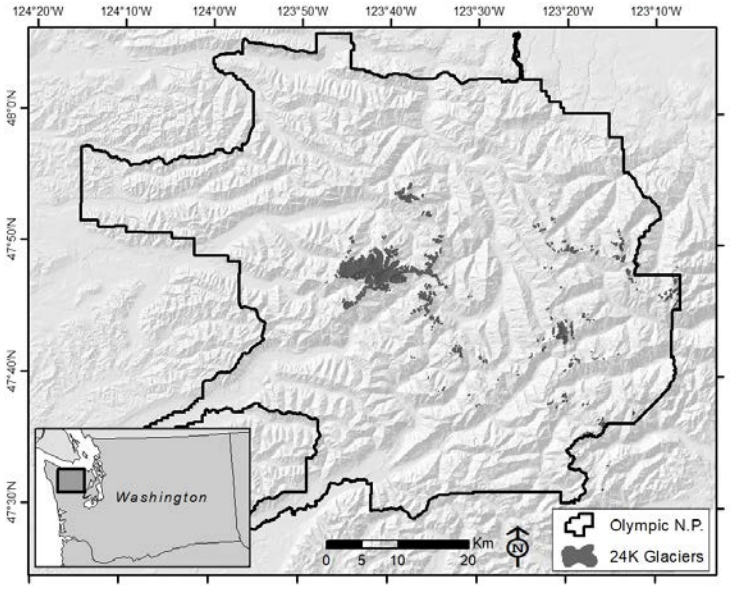

Figure 1. Location of the Olympic Peninsula and glaciers. The dark black line is the boundary of Olympic National Park. The gray outlined box surrounds Mt. Olympus.

Glaciers were first photographed in 1890 during a US Army Exploring Expedition (Spicer, 1989; Wood, 1976). One glacier, the Blue Glacier, became the focus of interest because it is the largest glacier in the region. During the International Geophysical Year in 1957 it was mapped and identified as one of the glaciers in western North America suitable for monitoring (AGS, 1960). In that same year a mass balance monitoring program was established and has continued intermittently (Armstrong, 1989; Conway et al., 1999; LaChapelle, 1959).

Spicer (1986) compiled the first detailed inventory of the region. He mapped the glaciers by modifying glacier outlines on US Geological Survey 1:36,360-scale topographic maps according to their extent on vertical aerial photographs (1:24,000 to 1:60,000) acquired in 1976, 1979, 1981, and 1982, and supported by field observations from 1980 - 1983. Ice masses were classified as glaciers if they persisted for at least two years; displayed evidence of glacier flow

such as crevasses, medial moraines, meltwater with glacier flour; or showed glacial activity such as terminal or lateral moraines.

Fountain et al. (2017) developed a second inventory of glaciers and perennial snowfields in the Olympic Mountains as part of a larger inventory that included the entire western US exclusive of Alaska. The outlines of this newer inventory were abstracted from US Geological Survey 1:24,000-scale topographic maps drawn from aerial photography flown in 1943, 1968, 1976, 1979, 1985, and 1987. Most glaciers (93%) were photographed during 1985-1987 and only a few in 1943. This inventory identified more glaciers (391) than Spicer (265) largely due to Spicer's 0.1 km^2 area threshold for inclusion, compared to the 0.01 km^2 adopted by Fountain et al. (2017). When the 0.1 km^2 threshold was applied to Fountain et al. (2017) the distributions of both inventories largely accord. Riedel et al. (2015) compiled a third inventory of glaciers based on aerial photography from 2009. One of the authors (Fountain) was involved with the compilation of this inventory the details of which are summarized in Methods below.

Our objectives are to provide a comprehensive examination of the glaciers in the Olympic Mountains, how they have changed in area and volume since the early 1980s to 2015, and how they responded to climatic variations since 1900. This report differs from Riedel et al. (2015) in several ways. First, we provide two new inventories and examine in detail how the populations change over time. We demonstrate that area changes of Blue Glacier are representative of the population as a whole and examine the precipitation and air temperature influences on Blue Glacier in the context of larger climate indices that represent hemispheric scale oceanic and atmospheric processes. Finally, we predict the future of glacier cover in the Olympics over the next century.

2. Methods

To assess the changing area and distribution of glaciers in the Olympic Mountains we relied on several previously published glacier inventories and created two new inventories. The first glacier inventory from Spicer (1986) provides the earliest detailed inventory, however, results

are in tabular form with approximate latitude and longitude locations. Newer inventories were compiled in a geographic information system as digital outlines of glaciers and perennial snowfields. Three new inventories were compiled for the Olympic Mountains using vertical aerial photographs flown in September of 1990, 2009, and 2015. The 1990 images are black and white digital orthoquadrangles (DOQs) with a ground resolution of 1 m. They were downloaded from the University of Washington Geomorphological Research Group webpage (UW, 2019). The 2009 and 2015 imagery were obtained from the U.S. Department of Agriculture (USDA) National Agricultural Imagery Program (NAIP) website (USDA, 2019) as 1 m color georectified orthophotographs. The 2009 inventory was reported in Riedel et al (2015). The 2015 imagery included all but 16 glaciers, which were outlined using WorldView-2 satellite imagery, 0.5 m spatial resolution obtained from Digital Globe and acquired in August and September (Gorelick et al., 2017). The comprehensive inventory of the continental US (Fountain et al., 2007, 2017) was not used because the original USGS imagery of the Olympic Mountains included extensive seasonal snow masking many of the glacier outlines. Also, the imagery dates are within a couple of years of Spicer's inventory rendering the inventory unnecessary.

The new inventories include both glaciers and perennial snowfields (G&PS) because they are often hard to distinguish when small and perennial snowfields can be locally important for late summer runoff (Clow & Sueker, 2000; Elder et al., 1991). Glaciers are identified by the presence of exposed ice and crevasses, indicating a perennial nature and movement, respectively. Snowfields, on the other hand, rarely provide visual clues regarding their perennial nature because their firn core is usually snow-covered in the imagery. We only track their persistent presence in the imagery. Given the episodic nature of suitable imagery over four decades these features cannot be tracked closely. Therefore, we adopt rules from (DeVisser & Fountain, 2015) to distinguish seasonal from perennial features. In short, if a feature is present in the first inventory (Spicer for glaciers, 1990 for snowfields) and not found in subsequent inventories it is considered seasonal and eliminated. If the feature is found in the first two inventories it is considered perennial, and if it is absent from any subsequent inventory it is considered no longer perennial. Outlines were digitized in ArcGIS (ArcMap, ESRI, Inc) at a scale of 1:2,000 with

vertices spaced at a 5 m interval. This approach balanced accuracy, productivity, and image resolution. The minimum area threshold was 0.01 km^2, consistent with Fountain et al. (2017) for the Western US, and global guidelines for glacier inventories (Paul et al., 2010). To insure internal consistency, the three new inventories were intercompared and any abrupt change in area initiated a reexamination of that G&PS outline.

Area uncertainty results from three sources, positional, digitizing, and interpretation (DeBEER & Sharp, 2009; DeVisser & Fountain, 2015). Positional uncertainty (U_p) is the error in the location of the perimeter caused by alignment of the base image during the orthorectification process. Digitizing uncertainty (U_d) results from inaccuracies in following the glacial perimeter during manual digitizing. Finally, interpretation uncertainty (U_i) is the location uncertainty of the glacier margin due to masking by seasonal snow cover, rock debris, or shadows. The total uncertainty (U_t) for each feature is the square root of the sum of the square of each contributing uncertainties (Baird, 1962).

$$U_t = \sqrt{U_p^2 + U_d^2 + U_i^2} \qquad (1)$$

To evaluate (1), we ignored positional uncertainty (U_p) because we are concerned with area not exact location. Furthermore, the digitized points are highly correlated such that they are not independently determined. To evaluate the digitization uncertainty (U_d), we follow (Hoffman et al., 2007) who adapted the method of (Ghilani, 2000). This uncertainty is a product of the length of the side of a square (S) that has the same area as the feature polygon in question multiplied by the linear uncertainty (σ_d),

$$U_d = S\sigma_d\sqrt{2} \qquad (2)$$

To estimate the linear uncertainty (σ_d). Ten features of various sizes were digitized at the normal 1:2000 scale and again at 1:500. The linear difference was measured perpendicularly between outlines and the standard deviation calculated. For interpretation uncertainty we tried

several approaches including, visual estimates (e.g. 5% of the area is in shadow, uncertainty is ±2.5%), measured glacier area with and without the questionable subregion using one half of the difference as the uncertainty, or a combination of both approaches where measurements were used to calibrate visual estimates. In most cases we found little difference between methods.

The uncertainty for snowfields was estimated differently. Snowfield area commonly changed dramatically (~ 50%) between imagery surveys, due to residual seasonal snow. Because its firn core was rarely observed uncertainty is unknown. To document the presence of perennial snowfields but eliminate them from analysis, a large uncertainty was estimated using a buffer around the outline such that the observed changes in area were smaller than the uncertainty.

To calculate the topographic characteristics of the initial, (Spicer, 1986) inventory, we used the original National Elevation Dataset based on the 1:24,000 paper maps (Gesch et al., 2002). Most of the mapping (94%) in the Olympics was based on aerial photography from 1980-1987 (Fountain et al., 2017). As will be shown later, during this period little glacier recession occurred and we consider the topography to be representative of the 1980 inventory.

Volume change was estimated by differencing surface elevations of the glaciers collected at different times. Two digital elevation models (DEMs) were used. The earlier DEM is the National Elevation Dataset and the more recent DEM is from aerial lidar collected in summer 2015 (Painter et al., 2016). Uncertainty was estimated by the root-mean square error of the elevation differences calculated for the snow-free bedrock adjacent to the glaciers.

The local climate of precipitation and maximum/minimum air temperatures was defined using Parameter-elevation Regression on Independent Slopes (PRISM) data (Daly et al., 2007). Monthly values were downloaded at a scale of 4 km within a box 10.7 km by 8.5 km, centered over Mt. Olympus (47.7986°, -123.693°) (OSU, 2017). To examine the influence of broader climate patterns climate indices were downloaded from a number of sources. For the Arctic

Oscillation (AO, Barnston and Livezey, 1987; Thompson and Wallace, 1998); Nino 3.4 (Bjerknes, 1966; Rayner et al., 2003; Trenberth, 1997); North Atlantic Oscillation (NAO, Jones et al., 1997); North Pacific index (Trenberth & Hurrell, 1994); Pacific-North American (PNA, Wallace & Gutzler, 1981), and the Southern Oscillation Index (Cayan, 1996; Chen, 1982; Ropelewski & Jones, 1987), the data were downloaded from the US National Oceanic and Atmospheric Administration, Earth System Research Laboratory, Physical Sciences Division (NOAA, 2018). The data for the Pacific Decadal Oscillation (PDO, Mantua & Hare, 2002; Newman et al., 2016), were downloaded from the University of Washington (UW, 2018). The period of correlation was 1900 – 2014 for all variables except Arctic Oscillation, which was 1950-2014 due to data availability. The correlations reported are for the longer period of record.

3. Results

The Spicer (1986) inventory identified 266 glaciers $\geq$ 0.01 km^2, most (94%) of which were identified from 1979-1982. During this period the glaciers changed little because it coincides with the mid-century cool period when glaciers were either in equilibrium or advancing slightly (Conway et al., 1999; Hodge et al., 1998; Thompson et al., 2010). For simplicity, the inventory is dated to 1980 and referred to as the '1980 inventory'. Our reanalysis revised the 1980 inventory to 261 glaciers because one glacier, White Glacier, was counted as two glaciers due to its split terminus into two lobes, and four other features were considered seasonal because they were missing from the following 1990 inventory. Total glacier area was 45.89 ± 0.51 km^2, of which almost half, 20.4 km^2, are located on the Olympus Massif. The largest glacier was Blue Glacier, 6.02 ± 0.30 km^2 and the smallest was an unnamed ice mass, 0.01 km^2. Average glacier area was 0.18 km^2 with a median of 0.05 km^2. The area of many glaciers cannot be quantified because Spicer's inventory often grouped small glaciers within the same watershed under a single identification number and summing their area. Mean glacier elevations range from 1319 m to 2399 m amsl with a mean elevation of 1726 m. The mean elevation of almost all glaciers (98%) was < 2000 m and 45% have a maximum elevation < 2000 m (Figure 2). Glaciers facing north (330^o to 30^o) account for 55.6% of the population and 52% (24.0 km^2) of the total area.

The glaciers were inventoried again using imagery from 1990, 2009, and 2015. These were the years with suitable late-summer imagery. The quality was good to excellent with moderate amounts of snow cover in some places. The summer of 2015 was a particularly low snow year and the alpine landscape was largely snow-free. The root mean square error of uncertainty for all outlines in each inventory was 1% of the total area. Forty-seven more G&PS were identified in the new inventories compared to the original 1980 glacier inventory. GIS methods and comparison between inventories more conclusively defined perennial features (Table 1).

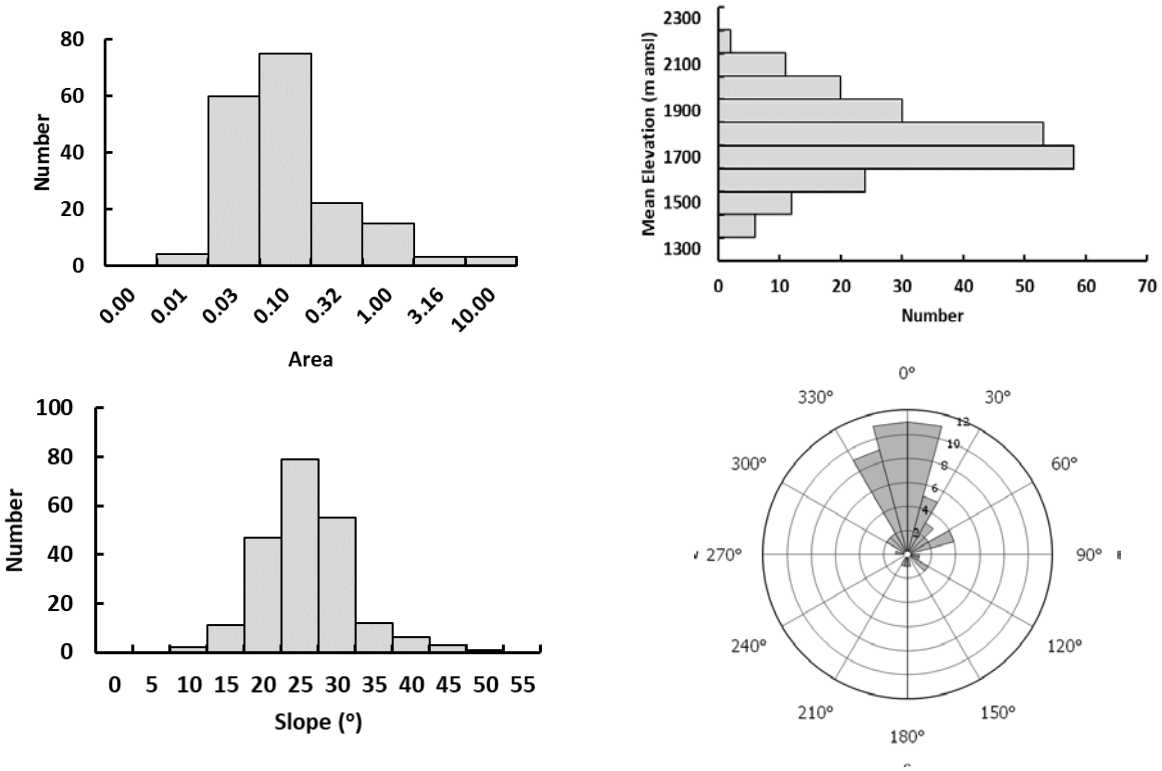

Figure 2. Topographic characteristics of the 1980 glacier inventory. Clockwise from upper left: Frequency distributions of glacier area, mean elevation, aspect, and mean slope. For bar graphs, the value of the bin is the maximum value for bin. For area, note the logarithmic values on the x-axis.

Tracking the glaciers originally identified by the 1980 inventory showed that by 2015, total glacier area decreased by -45% (-0.59 km^2 yr^{-1}), mean glacier area decreased from 0.18 km^2 to 0.10 km^2, and 35 glaciers disappeared (Table 1 Partial Inventory). The distribution of glacier area in 1980 approximates a normal distribution, but becomes increasingly skewed favoring smaller glaciers with time resulting in a highly skewed area-population distribution by 2015 (Figure 3). Given the close correspondence of fractional area change between the complete and partial inventories, we estimate that about 45% of the ice-covered area was lost between 1980 and 2015. A total of 51 G&PS in the complete inventory disappeared and 134 decreased below 0.01 km^2 (but > 0) , the minimum threshold for glacier inclusion (Fountain et al., 2017; Paul et al., 2010). These very small ice masses remain in the inventory given their perennial nature and their known history.

The time periods between inventories vary from 6 to 19 years, during which 19% - 37% of area changes were less than the uncertainty. During every time period total glacier area decreased, but with one to eight glaciers increased area greater than uncertainty. No glacier increased area for two or more consecutive time periods. The rate of total area change slowed from -0.66 km^2 yr^{-1} (1980-1990) to about -0.48 km^2 yr^{-1} (1990-2009) before accelerating again to -0.82 km^2 yr^{-1} (2009-2015). Of the G&PS that disappeared, most occurred in the last period, 1990-2009.

Table 1. Statistics for inventories of all glaciers and perennial snowfields found in the Olympic Mountains. The Complete Inventory summaries all glaciers found in each inventory and the Partial Inventory are those that are common to the 1980 inventory. For area and uncertainty (km^2), Max is maximum, Min is minimum, Med, is median area. Area change is the change since last inventory and can only be calculated for inventories that include the same populations; R Frc Chg is the relative fractional area change since previous inventory and is the change (and uncertainty) divided by the area of the previous inventory; T Frc Chg Is the total fractional change since the 1980 inventory; Rate Chg is the rate of area change in km^2 yr^{-1} based on the area change and years between inventories; Total Num is the number of glaciers and perennial snowfields in the inventory; Disappeared is the number that have vanished since last inventory. Uncertainty is included in smaller font, and is the root mean square error except for the

mean, which is the standard deviation. The 2009 inventory was originally published in Riedel et al (2015).

	1980		1990		2009		2015	
Complete Inventory								
Max Area	6.02	± 0.30	5.74	± 0.30	5.35	± 0.08	5.14	± 0.09
Min Area	0.01	± 0.00)	0.001	± 0.001	0.000	± 0.000	0.000	± 0.000
Mean Area	0.18	± 0.59	0.13	± 0.51	0.10	± 0.46	0.08	± 0.43
Med. Area	0.05		0.02		0.01		0.01	
Total Area	45.89	± 0.51	39.66	± 0.53	30.35	± 0.22	25.34	± 0.27
Area Chg					-9.31	± 0.58	-5.01	± 0.35
R. Frc. Chg					-0.23	± 0.01	-0.17	± 0.01
T. Frc. Chg					-0.23	± 0.01	-0.36	± 0.02
Rate Chg					-0.49	± 0.03	-0.84	± 0.06
Total Num	261		308		306		255	
Disappeared			0		2		51	
Partial Inventory								
Max Area	6.02	± 0.30	5.74	± 0.30	5.35	± 0.08	5.14	± 0.09
Min Area	0.01	± 0.00	0.001	± 0.001	0.000	± 0.000	0.000	± 0.000
Mean Area	0.18	± 0.59	0.15	± 0.55	0.12	± 0.49	0.10	± 0.47
Med. Area	0.05		0.03		0.02		0.01	
Tot. Area	45.89	± 0.51	39.31	± 0.53	30.16	± 0.22	25.25	± 0.27
Area Chg			-6.58	± 0.74	-9.15	± 0.58	-4.90	± 0.35
R. Frc. Chg			-0.14	± 0.02	-0.23	± 0.01	-0.16	± 0.01
T. Frc. Chg			-0.14	± 0.02	-0.34	± 0.01	-0.45	± 0.02
Rate Chg			-0.66		-0.48	± 0.03	-0.82	± 0.02
Total Num	261		261		259		226	
Disappeared			0		2		35	

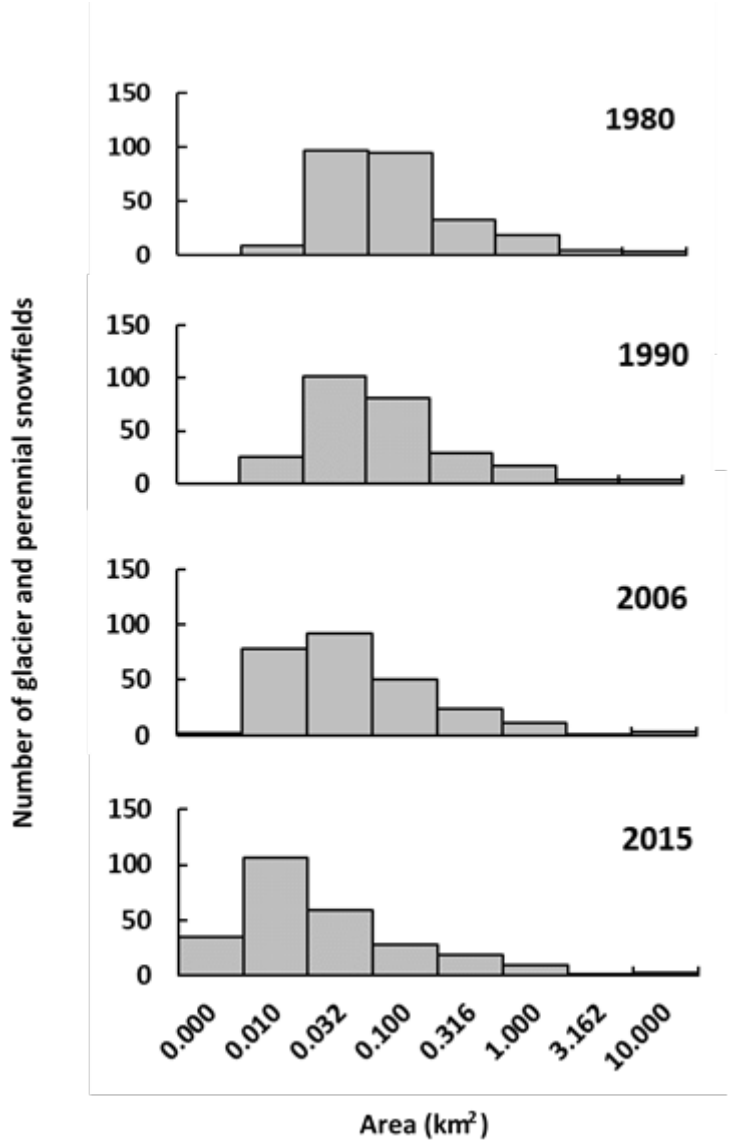

285

286 *Figure 3. The number of glaciers as a function of their area for each of the inventories. The*
287 *horizontal axis intervals are logarithmic increasing by a power of 0.5; tick labels on the x-axis*
288 *represents maximum bin value. The G&PS in the zero column are those that disappeared since*
289 *the previous inventory.*

290

291 **4. Analysis**

292

293 4.1 Effect of Topography

To examine the influence of topographic factors, such as elevation and aspect, on glacier area change, the change was first normalized by dividing by initial area yielding a fractional area change. Results show that smaller glaciers shrink proportionally more than larger glaciers but the variability of shrinkage is also much larger. Much of the variability in very small glaciers is probably due to local topographic effects, such as topographic shadowing by valley walls or local snow accumulation via avalanching and wind drift (Basagic & Fountain, 2011; DeBEER & Sharp, 2009; Kuhn, 1995). In contrast, local boundary conditions affect larger glaciers much less. In order to minimize boundary effects, the glaciers <0.1 km^2 were eliminated from the topographic analysis.

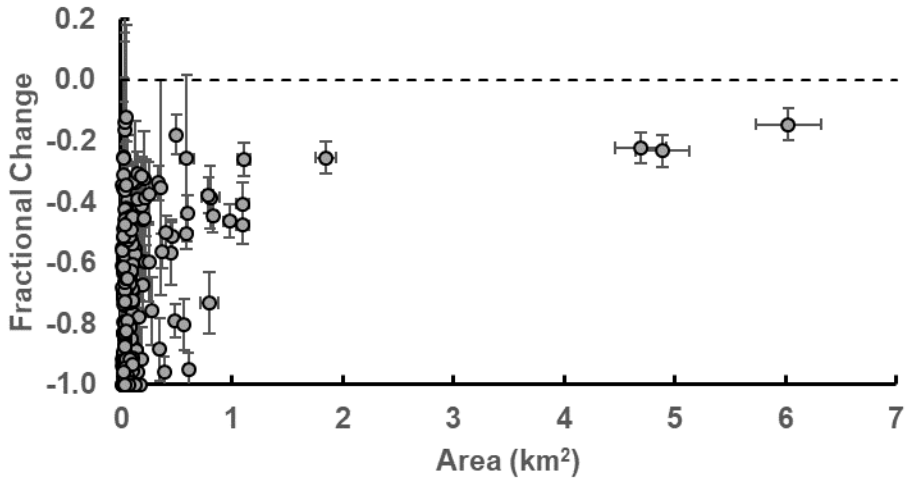

Figure 4. Fractional area change of the glaciers and perennial snowfields in the Olympic Mountains as a function of initial area from 1980 to 2015 using the only the glaciers identified in 1980.

No correlation of fractional area change was found with area, aspect, slope, distance from the Pacific Ocean, winter precipitation or average seasonal temperature (summer, winter). The only correlative factor was elevation (Figure 5). Area changes were further examined by sorting the entire data set, including the small G&PS, from greatest to least, then subdivided into four groups. The topographic and climatic characteristics of the group with the largest change (≥ -

92%) were compared to those of the smallest change (≤ -51%). Each group consisted of about 55 glaciers. For glaciers with the largest relative change, almost half (21) disappeared, had a lower maximum elevation (Δ -250 m). Although no significant differences were observed for the other variables, the glaciers with the largest fractional change tended to be smaller (mean of 0.06 km^2 versus 0.56 km^2), and warmer (Δ +0.7^oC) air temperature in summer and winter, consistent with a lower elevation (Table A1).

To examine the effect of the distribution of glacier area with elevation the hypsometry index was compared with fractional area change. The index is a ratio of the elevation differences between the maximum and median and the median and minimum (Jiskoot et al., 2009). For example, if the elevation difference above the median is smaller than below the median it implies a shallow broad accumulation zone compared to a longer, narrower ablation zone. We expected that glaciers with a greater elevation extent above the median than below exhibit less area change over time. No pattern was found; accounting for aspect, elevation, or local climate provided no improvement.

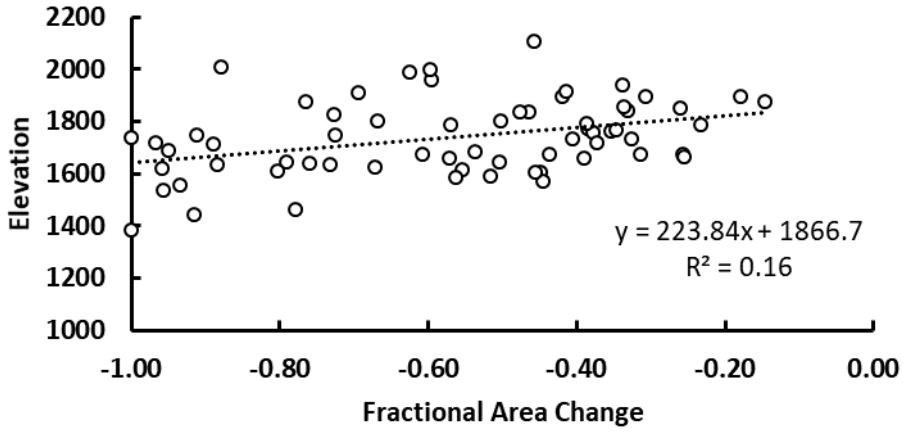

Figure 5. The factional area change (1980 to 2015) of glaciers and perennial snowfields (>0.1km^2) with elevation.

335 4.2 Volume Change

336

337 The SnowEx lidar surveyed 216 of 261 glaciers (83%) identified by 1980 inventory. In terms of
338 that inventory those 216 glaciers account for 43.0 km^2 (94%) of the total 45.9 km^2 area. The
339 estimated volume change between 1980 and 2015 is -0.694 $\pm$ 0.164 km^3 with a specific average
340 volume change of -16.1 $\pm$ 3.8 m. If this average is applied to the 45 glaciers not included in the
341 lidar survey, the total estimated volume change is -0.741 $\pm$ 0.164 km^3. No significant spatial
342 trends were observed with mean glacier elevation, slope, latitude, or longitude. If we assume
343 that all mass loss from storage occurs during the months of August and September, the period
344 in which seasonal snow is at a minimum and maximum ice is exposed, then the contribution to
345 stream runoff is about 347,000 $\pm$ 77,000 m^{-3} dy^{-1}.

346

347 We estimated the remaining ice volume in 2015 using an area – volume scaling relation (Bahr et
348 al., 2015). For glacier area, S, the volume, V, can be estimated as,

349

350 $$V = cS^{\gamma} \ , \qquad (1)$$

351

352 with c and γ as undefined parameters. We used parameter values from the literature including
353 those based on theoretical grounds (Bahr et al., 2015) and on empirical results (Chen &
354 Ohmura, 1990; Farinotti et al., 2009). Five estimates of volume were generated. The high and
355 low volume estimates were eliminated and the middle three were averaged, those included
356 Chen and Ohmura's (1990) categories of 'for the Cascades and other areas', 'for Cascades, small
357 glaciers'; and Farinotti et al., (2009), yielding, 0.75 ± 0.19 km^3. The uncertainty is the standard
358 deviation of the estimates. The Cascades refers to the mountain range ~100 km northeast of
359 the Olympics and it has a similar climate regime. From this estimate volume and the volume
360 change, the estimated total volume of all glaciers in 1980 is 1.49 ± 0.25 km^3.

361

362 4.3 Mt. Olympus

363

To investigate glacier change more closely we focus on the glaciers mantling Mt. Olympus, the highest peak (2,432 m) in the Olympic Mountains, representing 61% of the total glacier area in the region including the four largest glaciers and 6 of the 19 named glaciers. From 1980 to 2015, the glaciers lost about 0.42 km^3 (61% of total, Figure 6). The specific volume change for all glaciers was -20 ± 4 m, ranging from -30 ± 5 m (Humes Glacier) to -6 ± 4 m for one of the smaller unnamed glaciers. For Blue Glacier, the largest glacier, the specific volume change was -22 ± 4m.

The distribution of glacier area shifted to higher elevations, although the elevation of maximum area, 1700-1750 m, had not changed. (Figure 6). The fractional area change with elevation generally followed the fractional volume change with maximum change (decrease) at about 1500m. For elevations above about 1950 m, glacier area remained constant but thinned. Specific volume, above 1250 m shows a rapid decrease with elevation until about 1900 m where it reaches a relatively constant value of about -9 m. Below 1250 m glacier area is much smaller and some of it is debris-covered.

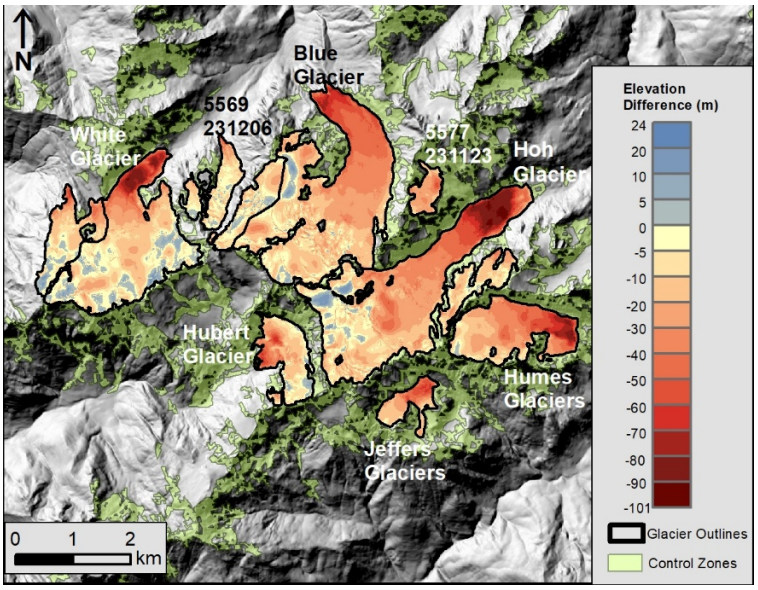
N
Blue Glacier
5569
231206
White Glacier
5577
231123
Hoh Glacier
Hubert Glacier
Humes Glaciers
Jeffers Glaciers
0 1 2 km
Elevation Difference (m)
24
20
10
5
0
-5
-10
-20
-30
-40
-50
-60
-70
-80
-90
-101
Glacier Outlines
Control Zones

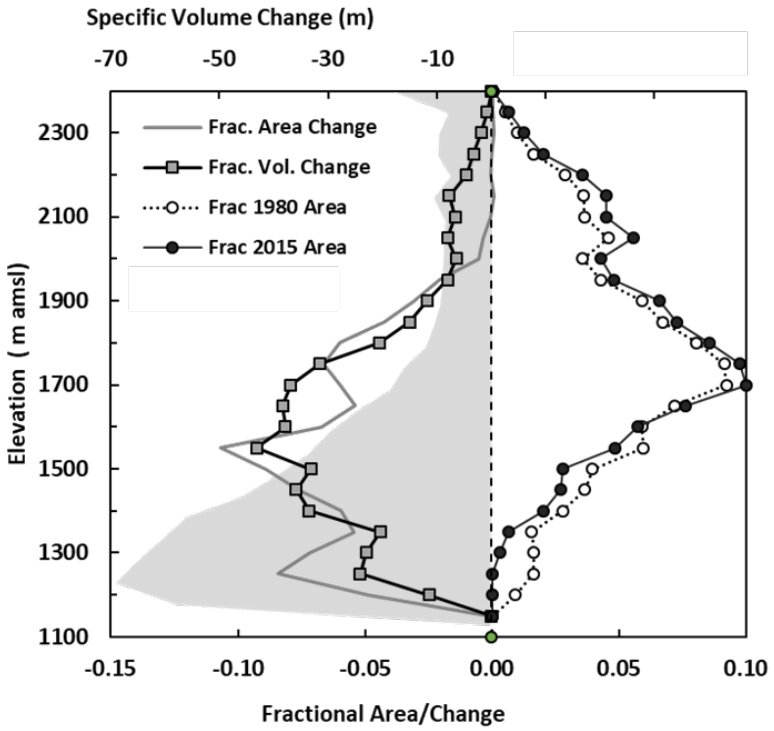
Specific Volume Change (m)
-70
-50
-30
-10
Frac. Area Change
Frac. Vol. Change
Frac 1980 Area
Frac 2015 Area
Elevation (m amsl)
2300
2100
1900
1700
1500
1300
1100
-0.15
-0.10
-0.05
0.00
0.05
0.10
Fractional Area/Change

380

381

382

Figure 6. Area and volume changes of the glaciers n Mount Olympus (1980-2015) as a function of elevation, in 50 m intervals. The top image shows the elevation change of all the glaciers. The numbers identify the unnamed glaciers, the 55XX is the record number of Fountain et al. (2017) and the 231XXX number is the hydroID of Spicer (1986)*. The bottom graph is the glacier change averaged over 50 m elevation bands. Frac is the fraction of total and Vol is volume. Specific volume change, shaded, is the volume change per unit area with an uncertainty of ± 4m.*

To test whether the changing glacier area on Mt. Olympus is representative of the other glaciers in the region the two were compared using the compiled inventories (Figure 7). Results show the two are highly correlated. The linear correlation suggests that should all the other glaciers disappear the area of those on Mt. Olympus shrinks to about 12.5 km^2.

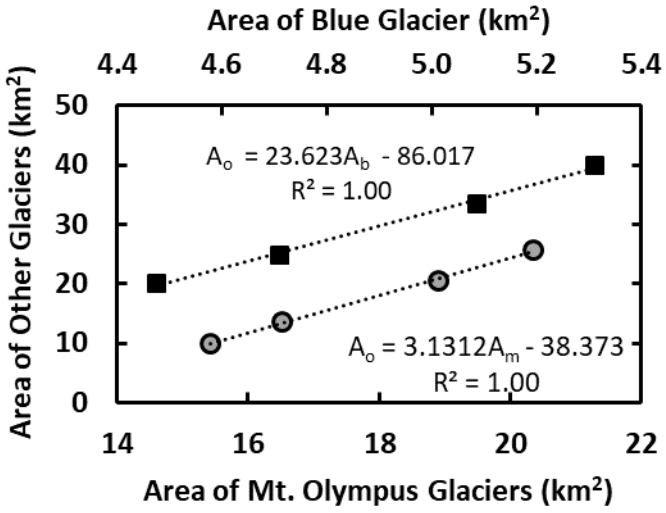

Figure 7. Area of all the glaciers in the region, except those on Mt. Olympus, plotted with respect to the area of the glaciers on Mt. Olympus (grey dots), and the area of all glaciers including those on Mt. Olympus, except Blue Glacier, plotted against the area of Blue Glacier alone (black squares). Linear regressions are shown. A_o is the area sum of all the other glaciers in the Olympic Mountains, not including those of the independent variable. A_m is the area of all glaciers on Mt. Olympus and A_b, the area of Blue Glacier.

The most extensively studied glacier in the Olympic Mountains is Blue Glacier, dating back to the late 1950s (Conway et al., 1999; LaChapelle, 1959; Rasmussen et al., 2000; Spicer, 1989). Because of this activity and interest, the glacier area has been well-documented over time (Figure 8). The pattern shows equilibrium for the first two decades of the 20th Century, followed by rapid retreat that ended in the middle 1940s. The glacier was stable/advancing slightly over the next 40 years, peaking in the early 1980's. Note the stability in the late 1970's to early 1980's, the period of time when the Spicer and the USGS were making glacier maps of the region. By the 1990's the glaciers were in rapid retreat continuing through to 2015. Based on the correlation shown in Figure 7, the changes in the glacier area for the Olympic Mountains should vary in a similar manner. The estimated total area in 1900 is 55.3 km^2, more than twice the 2015 area of 25.3 km^2.

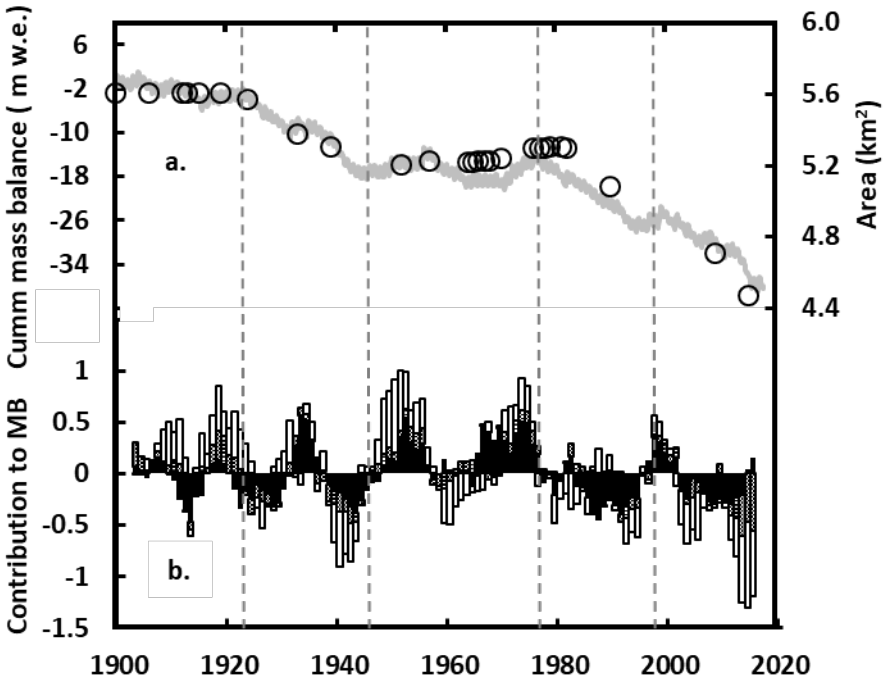

Figure 8. Changes of Blue Glacier and mass balance drivers. a. Area change of Blue Glacier since 1900 (circles) and estimated cumulative (cumm) monthly mass balance (grey line). Area data prior to 1990 from Spicer (1989), see Table A2. The vertical dashed lines are climate regime

shifts of the North Pacific 1923, 1946, 1977, and 1998 (see text). b. Contribution to the mass balance (MB) departures (5-year running mean) from winter accumulation (black), winter air temperature (white), and summer air temperature (cross hatched) departures

4.4 Climate Change and Glacier Mass Balance

The climate of the Olympic Mountains is maritime, with relatively warm winters with abundant precipitation followed by cool dry summers (Figure 9a). The accumulation and ablation seasons were defined using air temperature. Winter was defined for those months when the minimum and mean (average of the maximum and minimum) temperatures <0°C; and included December through March. Monthly maximum temperatures were commonly > 0°C. Summer was defined for those months in which the minimum temperatures were ≥0°C; and included May through October. The transition months are November and April. The net balance year nominally starts in November and ends in October.

To determine how temperature and precipitation has changed over the past century, the monthly averages of the first 50 years of record were subtracted from the monthly averages of the last 20 years (Figure 9b). For all months, the average air temperature warmed by +0.5°C and precipitation increased by +171 mm (+8%). Summer air temperatures warmed by +0.4°C and precipitation slightly decreased -8 mm (-1%); for winter, temperatures warmed by +0.7°C and precipitation increased by +47 mm (+2%). For specific months, monthly air temperatures warmed the most in midwinter (January, +1.8°C) and in mid-summer (August, +0.9°C). Precipitation changed little except for greater precipitation in October and November, months when the average air temperature is above freezing.

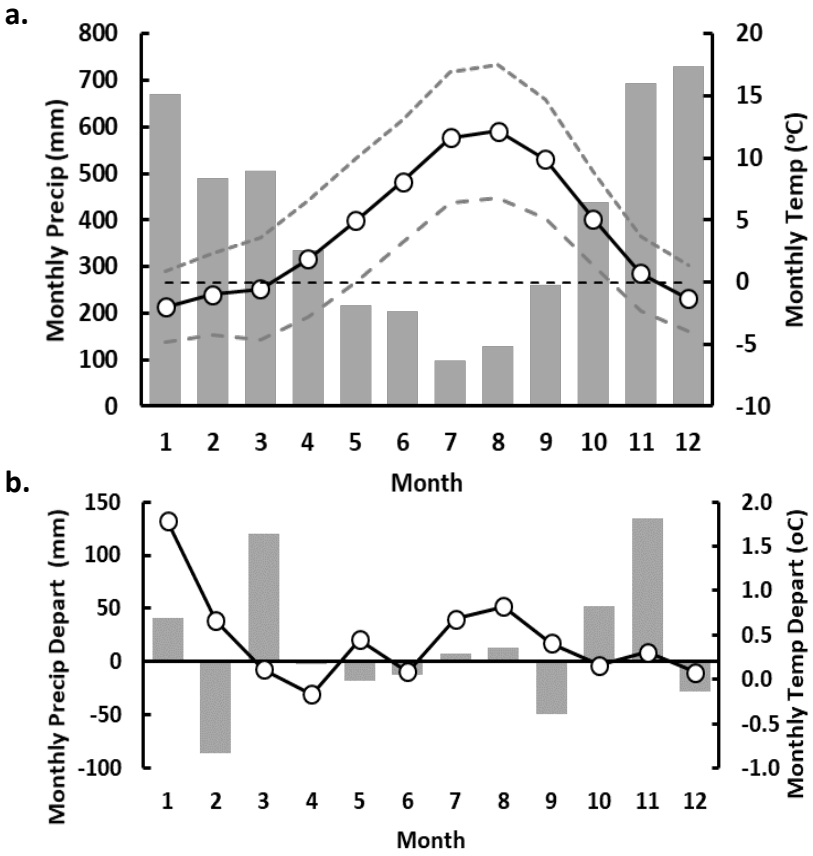

443 *Figure 9. Climate of the Mt. Olympus region from averaged monthly PRISM data* (Daly et al.,
444 2007)*, (a) over period 1900 – 2017. The bars represent precipitation (precip); the gray dashed*
445 *and black solid curves are minimum, mean, and maximum air temperature (temp). The mean is*
446 *an average of the maximum and minimum values. The fine horizontal dashed line represents*
447 *0°C. The second panel (b) are the departures in mean temperature and monthly precipitation*
448 *between the average of the first 50 years of record and the last 20 years.*
449
450 The time series of air temperature and precipitation show a century-scale warming trend for
451 both summer and winter temperatures but no trend in precipitation (Figure 10). At decadal
452 scales both temperature and precipitation vary. Warming winter temperature is particularly
453 important because it is already near 0°C and further warming changes the phase of
454 precipitation from snow to rain, reducing snowfall (mass gain) to the glaciers.

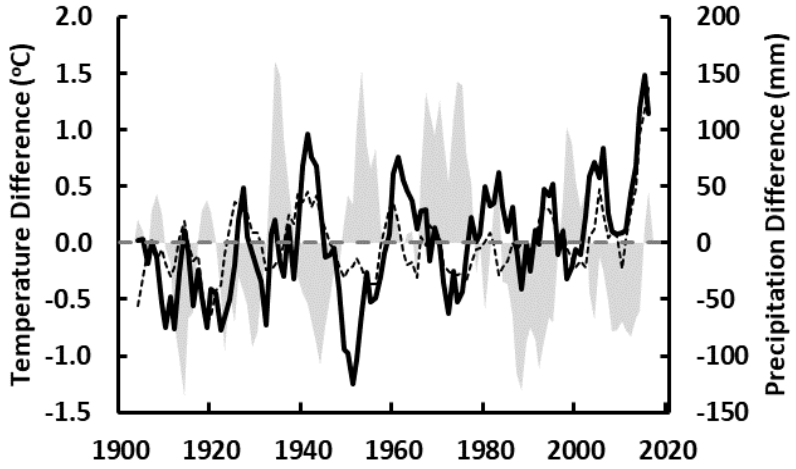

Figure 10. Difference from the mean (1900-2017) seasonal air temperature and precipitation, with a 5-year running mean applied, Mt Olympus, WA. The light solid grey is winter precipitation, the solid black line is winter temperature the dotted line is summer temperature.

To examine how glaciers in the Olympic Mountains respond to climatic variations we use Blue Glacier as a proxy because its area has been well-documented over the past century, its change correlates well with regional area changes, and mass balance has been measured at the glacier (Armstrong, 1989; Conway et al., 1999; LaChapelle, 1965). We use a simple model of glacier mass balance to provide a more direct link to climate, rather than observed changes in area that also responds to dynamic readjustment (Cuffey & Paterson, 2010). The model is simple and based on monthly PRISM values of precipitation and air temperature over the entire glacier (Daly et al., 2007; McCabe & Dettinger, 2002; McCabe & Fountain, 2013). Three adjustable parameters are required, two of which define the phase of precipitation for snow accumulation, the threshold temperatures for snowfall (≤ -2°C), and for rain (≥ +2°C). For temperatures between the snow/rain thresholds the ratio linearly changes from 1 to 0. Coincidently, Rasmussen et al (2000) found empirically that snowfall occurred in the accumulation zone of the glacier at air temperatures ≤ -2°C. One adjustable parameter is required to estimate ablation and defines the rate of melt as a function of air temperature. The monthly mass balance is then the sum of snow accumulation and ablation. We recognize the

limitations of this simple model, but use it here to understand the variations in mass balance, caused by changes in air temperature and precipitation, rather than for predictive values of mass balance.

Variations in the estimated mass balance closely matches the variations in glacier area over time (Figure 8). The cumulative mass balance over the period 1987-2015 is -17 m w.e. and compares favorably with the specific volume change -20 m w.e.± 4 m (-22 m ± 4 m elevation change) over the same period. Comparison with the estimated cumulative mass balance of Blue Glacier (1956-1997) by Conway et al. (1999), is good, although their mass balance increase in the 1980s was not apparent in our model. Comparisons to measured mass balances of five glaciers in the Cascade Range were also favorable in terms of synchronous change and magnitude (Riedel & Larrabee, 2016). Of the five glaciers the cumulative mass balance most closely resembled Sandalee Glacier.

Annual mass balance is best correlated with accumulation (R^2 = 0.98) and less so with the ablation (-0.79). Accumulation is correlated equally with winter air temperature (-0.61) and winter precipitation (+0.61). Ablation, as expected, is highly and inversely correlated with annual, winter, and summer temperatures (-0.98, -0.74, -0.84, respectively). Taken together, this is suggestive of the important role of air temperature in determining mass balance with precipitation playing a secondary role. To investigate the role of air temperature further, all variables were rescaled as mean standardized departures and a multiple linear regression was calculated to predict the model mass balance from annual air temperature and winter precipitation. The regression yielded a correlation coefficient of (R^2 = 0.85) and the correlation between the two independent variables was insignificant (R^2 = 0.001, p = 0.69). The relative importance of each independent variable on the mass balance was evaluated by multiplying the time series of each independent variable by its regression coefficient (McCabe & Wolock, 2009). Annual air temperature accounted for 83% of the variability in the root mean square value of mass balance whereas winter precipitation accounted for 53%. The regression was run again but with three independent variables, winter precipitation, summer air temperature and

winter air temperature, to define which seasonal air temperature was most influential. The regression yielded a slightly lower correlation (R^2= 0.82); and winter precipitation, summer, winter air temperatures accounted for 56%, 28%, and 68% of mass balance variability, respectively. Of the seasonal air temperatures, winter is more important. The time series of the contribution to the total mass balance departure was smoothed with a 5-year running mean and show that winter precipitation and winter air temperature vary most (Figure 8b). The mid-century cool period ~1946-1977 shows two episodes of cool winter air temperatures (positive departures of mass balance) simultaneously with two episodes of positive precipitation departures. The two episodes are separated by a warm winter period (negative mass balance departures) and average winter precipitation.

To examine the influence of broader climate patterns, monthly values of mass balance, air temperature, and precipitation were smoothed with a 12-month central running mean and correlated with the climate indices (Table A3). The highest correlations were found between the PDO, PNA, and NP with monthly air temperatures (R^2 = +0.53, +0.64, -0.58 respectively) and with mass balance (-0.52, -0.59, -0.56 respectively). Note that PDO, PNA, and NP are highly inter-correlated (e.g. PDO-PNA,+0.66; PNA-NP, -0.71) as are air temperature and mass balance (-0.74). Lesser correlations were found with Nino 3.4 and SOI for temperature (+0.52, -0.47), and for mass balance (-0.43, +0.40). Correlations between precipitation and the indices did not exceed ±0.19 and the correlation between air temperature and precipitation was also low, -0.12. Therefore, at annual time scales, PDO, PNA, and NP are the most influential atmospheric patterns on air temperature and mass balance.

The shifts in the mass balance of Blue Glacier coincide with regime shifts of sea surface temperatures in the North Pacific Ocean, which are typically related to the Pacific Decadal Oscillation PDO. Shifts occur in 1923, 1946, 1977, and 1998 (Figure 8) (Bond, 2003; Gedalof & Smith, 2001; Jo et al., 2015; Litzow & Mueter, 2014; Mantua & Hare, 2002; Minobe, 2002; Overland et al., 2008), and 1998 (Hare & Mantua, 2000; Jo et al., 2015; Minobe, 2002). No clear response is observed with the 1989 shift suggested by (Hare & Mantua, 2000). The periods of

glacier stability, 1890-1924, and 1947-1976 are associated with “cool” PDO regimes, whereas periods of glacier recession, 1925-1946, and 1977-1998, are associated with “warm” PDO regimes (Mantua and Hare, 2002). These data show that the mass balance of Blue Glacier specifically, and by implication those in the Olympic Mountains, are very sensitive to the sea temperatures conditions of the North Pacific.

5. The Glacier Future to 2100

To predict the future extent of the glaciers in the Olympic Mountains we applied the Regional Glaciation Model (RGM) developed by Clarke et al (2015) in modified form. The RGM is a distributed 2-dimensional, plan-view model. It grows glaciers from a bare-earth landscape at time steps of one year. The bare-earth landscape at 25m-scale digital elevation model is estimated by removing the glaciers identified by the Randolph Glacier Inventory using a surface inversion (Huss & Farinotti, 2012; Pfeffer et al., 2014). The final bare-earth landscape was rescaled to 100m. To drive the RGM model, monthly meteorological fields from a global climate model (GCM are downscaled. The Community Climate System Model 4 (CCSM4, Gent et al., 2011) generated these fields under various emission scenarios for the future. These scenarios are described as Regional Concentration Pathways (RCP, Van Vuuren et al., 2011) for different climate scenarios of low (2.6 W m^{-2} of additional forcing by 2100), moderate (4.5 W m^{-2}), or “business as usual” (8.5 W m^{-2}), respectively. The GCM simulations of air temperature, precipitation, and solar radiation are provided for grid cells 1^{o} x 1^{o} (latitude, longitude) and one cell covered the model domain. Spatial variation in air temperature and precipitation across the model domain was estimated using the Parameter-elevation Relationships on Independent Slopes Model (PRISM, Daly et al., 2007), an 800 m gridded data set based on weather station measurements and rescaled to 100m to match the digital elevation model. Monthly PRISM values, averaged over the period 1980-2010, subtracted from the GCM value, also averaged over the same period, producing a cell by cell offset for temperature and precipitation (Gray, 2019). We assume the spatial offsets do not change with time. The spatial pattern of solar radiation is calculated from the solar position at a constant solar angle for that month and the

562 value from the GCM is distributed accordingly. Finally, snow accumulates on the landscape
563 when precipitation occurs at air temperatures below 0^{o}C. Snow and ice melt are estimated
564 from a degree-day melt model and exposure to solar radiation.
565
566 Initial results showed that model could not predict the presence of glaciers in part of the
567 domain, east of Mount Olympus, despite extreme adjustments to the parameters. We
568 concluded that the source of the problem was snow accumulation through direct snowfall and
569 secondary sources of avalanching and wind redistribution. Significant uncertainty plagues
570 spatially distributed precipitation in mountainous regions (Gutmann et al., 2012; Livneh et al.,
571 2014). And secondary sources make important contributions to small glaciers (Frans et al.,
572 2018; Kuhn, 1995). Precipitation was increased by a factor of 3 over the footprint of the glaciers
573 producing reasonable results for glacier location and extent, similar to the approach of (Clarke
574 et al., 2015). Results showed the total area of modeled ice in 1980 was 106% of measured and
575 in 2015, 97%. About 60% of the glaciers were correctly placed. This mismatch is not of great
576 concern given the coarseness of the model, in terms of spatial resolution and approximation of
577 the mass balance processes.
578
579 Over time the model shows a dramatic loss of ice (Figure 11). For the RCP 8.5 “business as
580 usual” scenario shows that the glaciers will largely vanish by about 2070. With a moderate
581 reduction in greenhouse gases (RCP 4.5) the total glacier area will be reduced to a few km^2 at
582 most and limited to Mt. Olympus. The spikey character of the glacier area plot is typical of
583 widely dispersed small glaciers (Clarke et al., 2015).
584
585
586
587
588

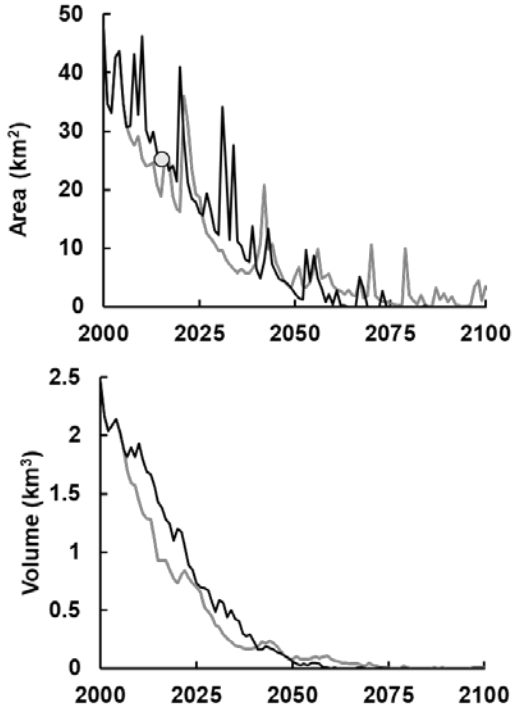

589

590 *Figure 11. Predicted area and volume for the glaciers of the Olympic Peninsula. The black line is*
591 *RCP 8.5 'business as usual' scenario, and the grey line is the RCP 4.5 modest reduction* (Van
592 Vuuren et al., 2011)*. The dot in the area plot is the measured glacier area in 2015.*

593

594 **6. DISCUSSION**

595

596 Our method of inventorying differed from the original inventory (Spicer, 1989) due to new
597 technology and digital imagery. This posed some challenges to developing a seamless series of
598 inventories over time. The methodological difference highlighted an important and often
599 overlooked issue. When updating an inventory completed by different authors, original
600 methods must be understood in order to minimize apparent changes in area resulting from
601 methodological differences (Paul et al., 2010; DeVisser and Fountain, 2015; Riedel and
602 Larrabee, 2016). This is also true for individual glaciers where interpretations of a glacier
603 boundary may differ dramatically between investigators. It is not so much a matter of boundary
604 interpretation as assumptions regarding which tributary or connected ice-covered landscape to
605 include. Imagery resolution is also important. Our new inventories were compiled from aerial

606 photographs or high-resolution satellite imagery both with a spatial resolution ≤ 1 m. This
607 resolution seemed suitable for outlining small glaciers (≥0.01 km^2) and certainly provides a
608 much better accuracy than 15 m resolution Landsat (Fischer et al., 2014). Also, compiling
609 inventories for more than one set of imagery is advantageous because although a single author
610 may compile the two new inventories some adjustment between inventories is required
611 because shifting assumptions during the data collection period. A second author complied the
612 last inventory and had to reconcile those outlines against the prior two inventories. This
613 minimized interpretation error over time.
614 The inventories are split into two categories. The partial inventories track only those 261
615 glaciers ≥ 0.1 km^2, identified in 1980 by Spicer (1986). The complete inventories, starting in
616 1990, include initially 308 glaciers and perennial snowfields ≥ 0.01 km^2. Although the
617 inventories differ by 47 features, the total areas did not differ by more than 0.35 km^2 and the
618 trend with time did not differ. To maintain the longest record the results from the partial
619 inventories are summarized.
620
621 The Olympic Mountains are populated by small glaciers, as of 2015 the average area was 0.08
622 km^2, and they have been shrinking over time like other regions in North America and elsewhere
623 globally (Abermann et al., 2009; DeBEER & Sharp, 2007; DeVisser & Fountain, 2015). Thirty-five
624 glaciers and 16 perennial snowfields have disappeared. The pattern of change is also similar
625 with the smaller glaciers exhibiting a wide range of shrinkage, but generally shrinking faster,
626 than the larger glaciers, which exhibit a smaller range of shrinkage (Bolch et al., 2010;
627 Granshaw & Fountain, 2006; Paul, 2004). The total area decreased by -45% since 1980 at a rate
628 of -1.3% yr^{-1}, faster than that for western Canada -0.6% yr^{-1} (1985-2000) (Bolch et al., 2010) and
629 faster than in the North Cascade Range 100 km to the northeast, -0.4% yr^{-1} (1959-2009) (Riedel
630 and Larrabee, 2016). However, as Bolch et al., (2010) point out this difference is probably due
631 to differences in glacier size because, as a general rule, smaller glaciers retreat faster than
632 larger glaciers. In addition, the glaciers in the Olympic Mountains are found at lower elevations
633 than most other regions. The retreat rate in the Olympics is more similar to the retreat rate of
634 small glaciers in western Canada such as on Vancouver Island (-1.11 % yr^{-1}), the Central Coast (-

635 1.2% yr^{-1}), or the Northern Interior (-1.11 % yr^{-1}). Our rate is also faster than glaciers in the
636 Wind River Range, Wyoming, USA (-0.65% yr^{-1}, 1966-2006), or the European Alps (-0.9% yr^{-1},
637 1970 – 2003) although Paul et al. (2011) argue for a rate of about 2% yr^{-1} from the mid-1980's
638 to 2003. In any case, the rate of retreat is within the range of other published studies.
639
640 Examination of topographic influences on glacier shrinkage showed that elevation was the only
641 significant influence, similar to other studies (DeVisser & Fountain, 2015). The scatter about the
642 regression line can be due to any number of factors including glacier hypsometry, aspect, and
643 slope (Fischer et al., 2015; Tangborn et al., 1990). A confounding factor is that smaller glaciers
644 generally retreat more than larger glaciers, and the retreat variability in much greater for
645 smaller glaciers (Figure 4; DeBEER & Sharp, 2007; Granshaw & Fountain, 2006; Paul, 2004). The
646 presence and change of small glaciers is highly dependent on the interrelation of topographic
647 and climatic factors (DeBEER & Sharp, 2009; Kessler et al., 2006; Kuhn, 1995). The absence of
648 hypsometric influence on the magnitude of area change may be due to the relatively small
649 glaciers that do not span a large elevation range so the climate differs little between the
650 terminus and head of the glacier.
651
652 The rate of specific volume changes averaged -0.46 m yr^{-1}, 1980-2015, and is comparable to the
653 mass change of the 30 global reference glaciers for the same time period (WGMS, 2019). Our
654 value is also close to that for the Olympic Mountains of -0.55 m yr^{-1} (2000-2015) estimated from
655 satellite imagery (Menounos et al., 2018) and to Riedel et al. (2015) of -0.54 m yr^{-1} (1980-2009)
656 based on aerial photographs. Using area-volume scaling, about 0.75 ± 0.19 km^3 of ice remains in
657 the Olympic Mountains as of 2015. Examining the changes on Mount Olympus, the largest
658 fraction of glacier-covered area is at 1750 m, but the maximum fractional volume change
659 (1980-2015) occurs 150 m lower at 1600 m amsl. This is the cross-over point between
660 decreasing specific volume change with elevation and increasing glacier-covered area. Such an
661 elevation offset is probably not unusual. Abermann et al. (2009) found similar results in Austria
662 for area change. Specific volume change no longer decreases with elevation above 2000 m,
663 becoming constant at -9 m. A similar result, -11 m (1985-1999), occurs for glaciers of British

Columbia, Canada (Schiefer et al., 2007). A constant thinning with elevation seems to occur at about 0.75 of the normalized elevation differences from the terminus to the glacier head in a number of regions (Arendt et al., 2006; Schiefer et al., 2007). The constant thinning at the upper-most elevations is similar to the constant mass balance at the upper-most elevations of individual glaciers and not a unique finding (Dyurgerov et al., 2002). The effect of altitude on ablation and accumulation can decrease significantly at high elevation due to cooler air temperatures, snowfall may decrease with elevation due to limits on cloud elevation, and high winds at elevation redistributes snow erasing an elevation dependence.

Based on the mass balance model of Blue Glacier, it is clear that variations in mass balance are highly sensitive to variations in air temperature (83% of the variability) and less so to variations in precipitation (53%), given their low elevation and high mass turnover. This is a known attribute of maritime glaciers (Anderson & Mackintosh, 2012; Oerlemans & Fortuin, 1992). Overall the retreat of these glaciers is due to increasing air temperatures over the past century, which has warmed by almost 1^{o}C in winter, which can change the phase of precipitation from snow to rain reducing mass accumulation and by about +0.3^{o}C in summer, which increases melt. The Olympic Mountains have been identified as one of the regions within the Pacific Northwest with warm snowpacks vulnerable to winter warming and increasing proportions of winter rain rather than snow (Klos et al., 2014; Nolin & Daly, 2006).

Of the climate indices correlated with monthly air temperatures and mass balance of Blue Glacier and therefore the glaciers of the Olympic Mountains, the PNA and PDO patterns were the strongest. PNA is a measure of the amplitude of the planetary wave field of atmospheric heights (pressures) over the northeast Pacific and North America at intramonthly time scales. It is correlated with freezing level in the atmosphere over western North America and most highly correlated over coastal Oregon and Washington (Abatzoglous, 2011). The PNA documents changes in atmospheric circulation, which contributes to wintertime warming and has been shown to correlate with snowpack generally in the western US (Barnston & Livezey, 1987; Cayan, 1996; Gutzler & Rosen, 1992). The impact of warming winter air temperatures on snow

accumulation in the western US has been described generally (McCabe & Wolock, 2009; Mote et al., 2005, 2018) and specifically for Blue Glacier (Rasmussen & Conway, 2000). Given that the mass balance of Blue Glacier is highly sensitive to air temperature correlation with the PNA index is not surprising. For PDO, the statistically significant correlation between temperature and mass balance is also reflective of conditions in the North Pacific. The PDO, based on sea surface temperatures, tends to vary over decadal time scales and is highly correlated with the PNA (Mantua and Hare, 2002; Newman et al., 2016). Like the PNA, the PDO is also correlated with snowpack variability such that positive PDO values, indicate warming along the coast of the Pacific Northwest and warmer air temperatures and reduced snow accumulation in the Pacific Northwest (McCabe & Dettinger, 2002; Zhang et al., 2010). It is striking that the shifts in the trend of mass balance of Blue Glacier are highly correlated with changes in the state of the Pacific Ocean, which is related to the PDO. They also largely explain the variation in winter mass accumulation estimated by Rasmussen & Conway (2000). The 'warm' phases of the PDO, where the ocean waters along the coast of western North America are warmer than normal, coincide with periods of decreasing mass balance whereas 'cool' phases are associated with the glacier mass balance in equilibrium or slightly gaining. This relationship has also been noted for Blue Glacier by Malcomb and Wiles (2013).

The response of glacier mass balance to climate indices in the Pacific Northwest have been well explored and show that the glacier mass balance is sensitive to conditions in the North Pacific Ocean (Bitz & Battisti, 1999; Hodge et al., 1998; Walters & Meier, 1989). Using the measured mass balance record from South Cascade Glacier, 150 km to the northeast of Blue Glacier in the Cascade Mountains, McCabe and Fountain (1995) showed that variations in in annual mass balance were driven by winter snow accumulation. From that Hodge et al., (1998) showed good correlations between winter mass balance and PNA; Bitz and Battisti (1999) showed good correlations with PDO and much less so with ENSO. McCabe and Fountain (1995) examined the correlations between the 700 mb atmospheric pressure field and the winter mass balance, finding a correlative pressure pattern across western North America similar to the PNA. Atmospheric circulation patterns that increase zonal westerly flow from the Pacific Ocean to

722 the Pacific Northwest have been shown to increase precipitation, particularly in high alpine
723 terrain (Luce et al., 2013; Menounos et al., 2018; Shea & Marshall, 2007). Increases in such
724 precipitation in winter, if air temperatures are below freezing, increase glacier mass balance.
725 However, increasingly warm winter climate since 2000 suggests that the cool phase of the PDO
726 is also becoming warmer reducing its ability to nourish the glaciers (Josberger et al., 2007).
727
728 The predicted demise of the glaciers by 2100 is not unique. Predictions of glacier change in
729 western Canada suggest a 70% volume loss by 2100 but for the Coastal Mountains of the
730 Central Coast and Vancouver Island, complete loss on or before 2100 (Clarke et al., 2015) (see
731 also supplementary material). This supports prior work in along the eastern slopes of the
732 Canadian Rocky Mountains and for selected glacier-populated basins in the Pacific Northwest
733 that are predicted to lose 80-90% of the glacier volume by 2100 (Frans et al., 2018; Marshall et
734 al., 2011). Predictions of global alpine glacier change suggest rapid loss for the rest of the
735 century and for the region of western Canada and US, exclusive of Alaska, at least 50% loss
736 (Radić & Hock, 2011).
737
738 **7. Conclusions**
739
740 Careful updating of prior glacier inventories is required to avoid introducing error based on
741 methodological differences or different assumptions regarding glacier boundaries. Glacier by
742 glacier comparisons between inventories minimized such errors.

743 The initial inventory of glaciers in the Olympic Mountains showed that the total area in 1980
744 was 45.9 ± 0.51 km^2 with a mean glacier area of 0.18 km^2. By 2015 the total area decreased -45
745 ± 0.02 %, mean glacier area decreased to 0.08 km^2, and 35 glaciers and 16 perennial snowfields
746 disappeared. Over this period glacier area decreased at a rate of -0.59 km^2 yr^{-1}, with the fastest
747 rate during the 2009-2015 period, -0.82 ± 0.02 km^2 yr^{-1}. Like other studies elsewhere, smaller
748 glaciers retreated more than larger glaciers, they also showed the most variability. The
749 variability is probably a result of favorable local conditions that decrease melt and increase
750 accumulation compared to less favorable conditions. To infer changes prior to 1980 we used

Blue Glacier, the largest (5.143 ± 0.094 km^2 in 2015) and most well documented glacier in the region, as a proxy for regional glacier change because of its high correlation with the regional area change. In 1900, the total area covered by glaciers was 55.3 km^2 more than twice the area in 2015.

A simple mass balance model of Blue Glacier, based on monthly air temperature and precipitation, showed good correspondence with changes in glacier area. Interrogation of the model showed that variations in monthly mass accumulation is better explained by variations in air temperature than precipitation, suggesting the importance of temperature control on the precipitation phase. Ablation is highly correlated with temperature alone. Taken together air temperature is the dominant influence on glacier mass balance in the Olympic Mountains, explaining 83% of the variance, with precipitation playing a secondary role. This is common to glaciers in maritime climates where winter air temperatures are close to the 0°C threshold and only a small change in temperature can change the phase of the precipitation from snow to rain. The mass changes are highly correlated with the Pacific North American index, a measure of the strength of zonal versus meridional air flow over North America at weekly-seasonal time scales. The changes are also correlated with regime shifts of the Pacific Decadal Oscillation, a measure of sea surface temperatures in the North Pacific that varies over decadal time scales. Finally, the future of these glaciers is grim. Using a coupled global circulation model with a distributed glacier flow model shows that the glaciers of the Olympic Mountains should largely disappear by 2070.

Acknowledgements

Supplementary Online Data can be found at, https://doi.org/10.15760/geology-data.02 The authors wish to acknowledge Steve Wilson who collected some of the early data and to Greg McCabe who provided very helpful comments on the climate section. This work was funded by the US Geological Survey via the Western Mountain Initiative.

Author Contributions

Andrew G. Fountain identified the goals and aims of the project, and participating in all phases of analysis and wrote the paper. Christina Gray applied the regional glaciation model to the

Olympic Mountains and edited the paper. Bryce Glenn created the 2015 glacier inventory and did the GIS analysis of glacier change, topography and climate across the region. Brian Menounos adapted the original formulation of regional glaciation model to include paleo GCM input, helped with preparing datasets for model inclusion, advised Christina on model implementation, and helped with the editing. Justin Pflug supplied the 2015 DEM data used for estimating glacier volume change and helped edit the paper. Jon Riedel supplied some of the glacier area data prior to 2015 and helped edit the paper.

References

Abermann, J., Lambrecht, A., Fischer, A., & Kuhn, M. (2009). Quantifying changes and trends in glacier area and volume in the Austrian Ötztal Alps (1969–1997–2006). *The Cryosphere Discussions*, *3*(2), 415–441. https://doi.org/10.5194/tc-3-205-2009

Abatzoglou, J. T. (2011). Influence of the PNA on declining mountain snowpack in the Western United States. International Journal of Climatology, 31(8), 1135–1142. https://doi.org/10.1002/joc.2137

AGS. (1960). *Nine Glacier Maps, Northwestern North America: Accompanied by Nine Separate Map Sheets on Scale of 1: 10,000*. American Geographical Society, Vol. 34, Lane Press.

Anderson, B., & Mackintosh, A. (2012). Controls on mass balance sensitivity of maritime glaciers in the Southern Alps, New Zealand: The role of debris cover. *Journal of Geophysical Research*, *117*(F1). https://doi.org/10.1029/2011JF002064

Arendt, A., Echelmeyer, K., Harrison, W., Lingle, C., Zirnheld, S., Valentine, V., Ritchie, B., & Druckenmiller, M. (2006). Updated estimates of glacier volume changes in the western Chugach Mountains, Alaska, and a comparison of regional extrapolation methods. *Journal of Geophysical Research*, *111*(F3). https://doi.org/10.1029/2005JF000436

Armstrong, R. L. (1989). Mass balance history of Blue Glacier, Washington, USA. In J. Oerlemans (Ed.), *Glacier Fluctuations and Climatic Change* (pp. 183–192). Springer Netherlands.

Bahr, D. B., Pfeffer, W. T., & Kaser, G. (2015). A review of volume-area scaling of glaciers: Volume-Area Scaling. *Reviews of Geophysics*, *53*(1), 95–140. https://doi.org/10.1002/2014RG000470

Baird, D. C. (1962). *Experimentation: An introduction to measurement theory and experiment design*. Prentice Hall. https://doi.org/0-13-295345-5

Barnston, A. G., & Livezey, R. E. (1987). Classification, seasonality and persistence of low-frequency atmospheric circulation patterns. *Monthly Weather Review*, *115*(6), 1083–1126. https://doi.org/10.1175/1520-0493(1987)115<1083:CSAPOL>2.0.CO;2

Basagic, H. J., & Fountain, A. G. (2011). Quantifying 20th Century Glacier Change in the Sierra Nevada, California. *Arctic, Antarctic, and Alpine Research*, *43*(3), 317–330. https://doi.org/10.1657/1938-4246-43.3.317

Bitz, C. M., & Battisti, D. S. (1999). Interannual to Decadal Variability in Climate and the Glacier Mass Balance in Washington, Western Canada, and Alaska. *Journal of Climate*, *12*(11), 3181–3196. https://doi.org/10.1175/1520-0442(1999)012<3181:ITDVIC>2.0.CO;2

Bjerknes, J. (1966). A possible response of the atmospheric Hadley circulation to equatorial anomalies of ocean temperature. *Tellus*, *18*(4), 820–829. https://doi.org/10.3402/tellusa.v18i4.9712

Bolch, T., Menounos, B., & Wheate, R. (2010). Landsat-based inventory of glaciers in western Canada, 1985–2005. *Remote Sensing of Environment*, *114*(1), 127–137. https://doi.org/10.1016/j.rse.2009.08.015

Bond, N. A. (2003). Recent shifts in the state of the North Pacific. *Geophysical Research Letters*, *30*(23). https://doi.org/10.1029/2003GL018597

Cayan, D. R. (1996). Interannual Climate Variability and Snowpack in the Western United States. *Journal of Climate*, *9*(5), 928–948. https://doi.org/10.1175/1520-0442(1996)009<0928:ICVASI>2.0.CO;2

Chen, J., & Ohmura, A. (1990). Estimation of Alpine glacier water resources and their change since the 1870s. *IAHS Publ*, *193*, 127–135.

Chen, W. (1982). Assessment of Southern Oscillation sea-level pressure indices. *Monthly Weather Review*, *110*(7), 800–807. https://doi.org/10.1175/1520-0493(1982)110<0800:AOSOSL>2.0.CO;2

Clarke, G. K. C., Jarosch, A. H., Anslow, F. S., Radić, V., & Menounos, B. (2015). Projected deglaciation of western Canada in the twenty-first century. *Nature Geoscience*. https://doi.org/10.1038/ngeo2407

Clow, D. W., & Sueker, J. K. (2000). Relations between basin characteristics and stream water chemistry in alpine/subalpine basins in Rocky Mountain National Park, Colorado. *Water Resources Research*, *36*(1), 49–61. https://doi.org/10.1029/1999WR900294

Conway, H., Rasmussen, L. A., & Marshall, H. P. (1999). Annual mass balance of Blue Glacier, USA: 1955-97. *Geografiska Annaler: Series A, Physical Geography*, *81*(4), 509–520. https://doi.org/10.1111/1468-0459.00080

Cuffey, K. M., & Paterson, W. S. B. (2010). *The Physics of Glaciers* (4th ed.). Academic Press.

Daly, C., Smith, J. W., Smith, J. I., & McKane, R. B. (2007). High-Resolution Spatial Modeling of Daily Weather Elements for a Catchment in the Oregon Cascade Mountains, United States. *Journal of Applied Meteorology and Climatology*, *46*(10), 1565–1586. https://doi.org/10.1175/JAM2548.1

DeBEER, C. M., & Sharp, M. J. (2007). Recent changes in glacier area and volume within the southern Canadian Cordillera. *Annals of Glaciology*, *46*(1), 215–221. https://doi.org/10.3189/172756407782871710

DeBEER, C. M., & Sharp, M. J. (2009). Topographic influences on recent changes of very small glaciers in the Monashee Mountains, British Columbia, Canada. *Journal of Glaciology*, *55*(192), 691–700. https://doi.org/10.3189/002214309789470851

DeVisser, M. H., & Fountain, A. G. (2015). A century of glacier change in the Wind River Range, WY. *Geomorphology*, *232*, 103–116. https://doi.org/10.1016/j.geomorph.2014.10.017

Dyurgerov, M., Meier, M., & Armstrong, R. L. (2002). *Glacier mass balance and regime: Data of measurements and analysis*. Institute of Arctic and Alpine Research, University of Colorado Boulder,, USA. ftp://sidads.colorado.edu/DATASETS/NOAA/G10002/Occasional_Paper55/instaar_occasional_paper_no55.pdf

Elder, K., Dozier, J., & Michaelsen, J. (1991). Snow accumulation and distribution in an alpine watershed. *Water Resources Research*, *27*(7), 1541–1552. https://doi.org/10.1029/91WR00506

Farinotti, D., Huss, M., Bauder, A., Funk, M., & Truffer, M. (2009). A method to estimate the ice volume and ice-thickness distribution of alpine glaciers. *Journal of Glaciology*, *55*(191), 422–430. https://doi.org/10.3189/002214309788816759

Fischer, M., Huss, M., & Hoelzle, M. (2015). Surface elevation and mass changes of all Swiss glaciers 1980–2010. *The Cryosphere*, *9*(2), 525–540. https://doi.org/10.5194/tc-9-525-2015

Fischer, Mauro, Huss, M., Barboux, C., & Hoelzle, M. (2014). The New Swiss Glacier Inventory SGI2010: Relevance of Using High-Resolution Source Data in Areas Dominated by Very

Small Glaciers. *Arctic, Antarctic, and Alpine Research*, *46*(4), 933–945. https://doi.org/10.1657/1938-4246-46.4.933

Fountain, A. G., Glenn, B., & Basagic, H. J. (2017). The Geography of Glaciers and Perennial Snowfields in the American West. *Arctic, Antarctic, and Alpine Research*, *49*(3), 391–410. https://doi.org/10.1657/AAAR0017-003

Fountain, A. G., Hoffman, M. J., Jackson, K., Basagic, H. J., Nylen, T. H., & Percy, D. (2007). *Digital outlines and the topography of the Glaciers of the American West* (Open File Report No. 2006–1340; p. 23). US Geological Survey. https://doi.org/10.3133/ofr20061340

Frans, C., Istanbulluoglu, E., Lettenmaier, D. P., Fountain, A. G., & Riedel, J. (2018). Glacier Recession and the Response of Summer Streamflow in the Pacific Northwest United States, 1960-2099. *Water Resources Research*. https://doi.org/10.1029/2017WR021764

Gedalof, Z., & Smith, D. J. (2001). Interdecadal climate variability and regime-scale shifts in Pacific North America. *Geophysical Research Letters*, *28*(8), 1515–1518. https://doi.org/10.1029/2000GL011779

Gent, P. R., Danabasoglu, G., Donner, L. J., Holland, M. M., Hunke, E. C., Jayne, S. R., Lawrence, D. M., Neale, R. B., Rasch, P. J., & Vertenstein, M. (2011). The community climate system model version 4. *Journal of Climate*, *24*(19), 4973–4991. https://doi.org/10.1175/2011JCLI4083.1

Gesch, D., Oimoen, M., Greenlee, S., Nelson, C., Steuck, M., & Tyler, D. (2002). The national elevation dataset. *Photogrammetric Engineering and Remote Sensing*, *68*(1), 5–32.

Ghilani, C. D. (2000). Demystifying area uncertainty: More or less. *Surveying and Land Information Systems*, *60*(3), 177–182.

Gorelick, N., Hancher, M., Dixon, M., Ilyushchenko, S., Thau, D., & Moore, R. (2017). Google Earth Engine: Planetary-scale geospatial analysis for everyone. *Remote Sensing of Environment*, *202*, 18–27. https://doi.org/10.1016/j.rse.2017.06.031

Granshaw, F. D., & Fountain, A. G. (2006). Glacier change (1958–1998) in the North Cascades National Park Complex, Washington, USA. *Journal of Glaciology*, *52*(177), 251–256. https://doi.org/10.3189/172756506781828782

Gutmann, E. D., Rasmussen, R. M., Liu, C., Ikeda, K., Gochis, D. J., Clark, M. P., Dudhia, J., & Thompson, G. (2012). A comparison of statistical and dynamical downscaling of winter precipitation over complex terrain. *Journal of Climate*, *25*(1), 262–281. https://doi.org/10.1175/2011JCLI4109.1

Gutzler, D. S., & Rosen, R. D. (1992). Interannual Variability of Wintertime Snow Cover across the Northern Hemisphere. *Journal of Climate*, *5*(12), 1441–1447. https://doi.org/10.1175/1520-0442(1992)005<1441:IVOWSC>2.0.CO;2

Hare, S. R., & Mantua, N. J. (2000). Empirical evidence for North Pacific regime shifts in 1977 and 1989. *Progress in Oceanography*, *47*(2–4), 103–145. https://doi.org/10.1016/S0079-6611(00)00033-1

Hodge, S. M., Trabant, D. C., Krimmel, R. M., Heinrichs, T. A., March, R. S., & Josberger, E. G. (1998). Climate variations and changes in mass of three glaciers in western North America. *Journal of Climate*, *11*(9), 2161–2179. https://doi.org/10.1175/1520-0442(1998)011<2161:CVACIM>2.0.CO;2

Hoffman, M. J., Fountain, A. G., & Achuff, J. M. (2007). 20th-century variations in area of cirque glaciers and glacierets, Rocky Mountain National Park, Rocky Mountains, Colorado, USA. *Annals of Glaciology*, *46*(1), 349–354. https://doi.org/10.3189/172756407782871233

Huss, M., & Farinotti, D. (2012). Distributed ice thickness and volume of all glaciers around the globe. *Journal of Geophysical Research*, *117*(F4). https://doi.org/10.1029/2012JF002523

Jiskoot, H., Curran, C. J., Tessler, D. L., & Shenton, L. R. (2009). Changes in Clemenceau Icefield and Chaba Group glaciers, Canada, related to hypsometry, tributary detachment, length–slope and area–aspect relations. *Annals of Glaciology*, *50*(53), 133–143.). https://doi.org/10.3189/172756410790595796

Jo, H.-S., Yeh, S.-W., & Lee, S.-K. (2015). Changes in the relationship in the SST variability between the tropical Pacific and the North Pacific across the 1998/1999 regime shift. *Geophysical Research Letters*, *42*(17), 7171–7178. https://doi.org/10.1002/2015GL065049

Jones, P. D., Jonsson, T., & Wheeler, D. (1997). Extension to the North Atlantic Oscillation using early instrumental pressure observations from Gibraltar and South-west Iceland. *International Journal of Climatology*, *17*, 1433–1450. https://doi.org/10.1002/(SICI)1097-0088(19971115)17:13<1433::AID-JOC203>3.0.CO;2-P

Josberger, E. G., Bidlake, W. R., March, R. S., & Kennedy, B. W. (2007). Glacier mass-balance fluctuations in the Pacific Northwest and Alaska, USA. *Annals of Glaciology*, *46*, 291–296. https://doi.org/10.3189/172756407782871314

940 Kessler, M. A., Anderson, R. S., & Stock, G. M. (2006). Modeling topographic and climatic
941 control of east-west asymmetry in Sierra Nevada glacier length during the Last Glacial
942 Maximum. *Journal of Geophysical Research*, *111*(F2).
943 https://doi.org/10.1029/2005JF000365
944 Klos, P. Z., Link, T. E., & Abatzoglou, J. T. (2014). Extent of the rain-snow transition zone in the
945 western U.S. under historic and projected climate: Climatic rain-snow transition zone.
946 *Geophysical Research Letters*, *41*(13), 4560–4568.
947 https://doi.org/10.1002/2014GL060500
948 Kuhn, M. (1995). The mass balance of very small glaciers. *Zeitschrift Fur Gletscherkunde Und*
949 *Glazialgeologie*, *5*, 171–179.
950 LaChapelle, E. (1959). Annual mass and energy exchange on the Blue Glacier. *Journal of*
951 *Geophysical Research*, *64*(4), 443–449. https://doi.org/10.1029/JZ064i004p00443
952 LaChapelle, Edward. (1965). Mass Budget of Blue Glacier, Washington. *Journal of Glaciology*,
953 *5*(41), 609–623. https://doi.org/10.3189/S0022143000018633
954 Litzow, M. A., & Mueter, F. J. (2014). Assessing the ecological importance of climate regime
955 shifts: An approach from the North Pacific Ocean. *Progress in Oceanography*, *120*, 110–
956 119. https://doi.org/10.1016/j.pocean.2013.08.003
957 Livneh, B., Deems, J. S., Schneider, D., Barsugli, J. J., & Molotch, N. P. (2014). Filling in the gaps:
958 Inferring spatially distributed precipitation from gauge observations over complex
959 terrain. *Water Resources Research*, *50*(11), 8589–8610.
960 https://doi.org/10.1002/2014WR015442

961 Luce, C. H., Abatzoglou, J. T., & Holden, Z. A. (2013). The Missing Mountain Water: Slower
962 Westerlies Decrease Orographic Enhancement in the Pacific Northwest USA. *Science*,
963 *342*(6164), 1360–1364. https://doi.org/10.1126/science.1242335
964 Malcomb, N. L., & Wiles, G. C. (2013). Tree-ring-based reconstructions of North American
965 glacier mass balance through the Little Ice Age—Contemporary warming transition.
966 *Quaternary Research*, *79*(2), 123–137. https://doi.org/10.1016/j.yqres.2012.11.005
967 Mantua, N. J., & Hare, S. R. (2002). The Pacific decadal oscillation. *Journal of Oceanography*,
968 *58*(1), 35–44. https://doi.org/10.1023/A:1015820616384
969 Marshall, S. J., White, E. C., Demuth, M. N., Bolch, T., Wheate, R., Menounos, B., Beedle, M. J.,
970 & Shea, J. M. (2011). Glacier Water Resources on the Eastern Slopes of the Canadian
971 Rocky Mountains. *Canadian Water Resources Journal*, *36*(2), 109–134.
972 https://doi.org/10.4296/cwrj3602823
973 McCabe, G. J., & Dettinger, M. D. (2002). Primary modes and predictability of year-to-year
974 snowpack variations in the western United States from teleconnections with Pacific
975 Ocean climate. *Journal of Hydrometeorology*, *3*(1), 13–25.
976 https://doi.org/10.1175/1525-7541(2002)003<0013:PMAPOY>2.0.CO;2
977 McCabe, G. J., & Fountain, A. G. (1995). Relations between atmospheric circulation and mass
978 balance of South Cascade Glacier, Washington, USA. *Arctic and Alpine Research*, *27*(3),
979 226–233. https://doi.org/10.1080/00040851.1995.12003117
980 McCabe, G. J., & Fountain, A. G. (2013). Glacier variability in the conterminous United States
981 during the twentieth century. *Climatic Change*, *116*(3–4), 565–577.
982 https://doi.org/10.1007/s10584-012-0502-9

McCabe, G. J., & Wolock, D. M. (2009). Recent Declines in Western U.S. Snowpack in the Context of Twentieth-Century Climate Variability. *Earth Interactions*, *13*(12), 1–15. https://doi.org/10.1175/2009EI283.1

Menounos, B., Hugonnet, R., Shean, D., Gardner, A., Howat, I., Berthier, E., Pelto, B., Tennant, C., Shea, J., Noh, M., Brun, F., & Dehecq, A. (2018). Heterogeneous changes in western North American glaciers linked to decadal variability in zonal wind strength. *Geophysical Research Letters*. https://doi.org/10.1029/2018GL080942

Minobe, S. (2002). Interannual to interdecadal changes in the Bering Sea and concurrent 1998/99 changes over the North Pacific. *Progress in Oceanography*, *55*(1–2), 45–64. https://doi.org/10.1016/S0079-6611(02)00069-1

Mote, P. W., Hamlet, A. F., Clark, M. P., & Lettenmaier, D. P. (2005). Declining mountain snowpack in western North America. *Bulletin of the American Meteorological Society*, *86*(1), 39–49. https://doi.org/10.1175/BAMS-86-1-39

Mote, P. W., Li, S., Lettenmaier, D. P., Xiao, M., & Engel, R. (2018). Dramatic declines in snowpack in the western US. *Climate and Atmospheric Science*, *1*(1). https://doi.org/10.1038/s41612-018-0012-1

Newman, M., Alexander, M. A., Ault, T. R., Cobb, K. M., Deser, C., Di Lorenzo, E., Mantua, N. J., Miller, A. J., Minobe, S., & Nakamura, H. (2016). The Pacific decadal oscillation, revisited. *Journal of Climate*, *29*(12), 4399–4427. https://doi.org/10.1175/JCLI-D-15-0508.1

NOAA (2018). www.esrl.noaa.gov/psd/gcos_wgsp/Timeseries/ Accessed, August 2018

Nolin, A. W., & Daly, C. (2006). Mapping “at risk” snow in the Pacific Northwest. *Journal of Hydrometeorology*, *7*(5), 1164–1171. https://doi.org/10.1175/JHM543.1

Oerlemans, J., & Fortuin, J. (1992). Sensitivity of glaciers and small ice caps to greenhouse warming. *Science*, *258*(5079), 115–117. https://doi.org/10.1126/science.258.5079.115

OSU, 2017. www.prism.oregonstate.edu, accessed November 2017.

Overland, J., Rodionov, S., Minobe, S., & Bond, N. (2008). North Pacific regime shifts: Definitions, issues and recent transitions. *Progress in Oceanography*, *77*(2–3), 92–102. https://doi.org/10.1016/j.pocean.2008.03.016

Painter, T. H., Berisford, D. F., Boardman, J. W., Bormann, K. J., Deems, J. S., Gehrke, F., Hedrick, A., Joyce, M., Laidlaw, R., Marks, D., Mattmann, C., McGurk, B., Ramirez, P., Richardson, M., Skiles, S. M., Seidel, F. C., & Winstral, A. (2016). The Airborne Snow Observatory: Fusion of scanning lidar, imaging spectrometer, and physically-based modeling for mapping snow water equivalent and snow albedo. *Remote Sensing of Environment*, *184*, 139–152. https://doi.org/10.1016/j.rse.2016.06.018

Paul, F., Frey, H., & Le Bris, R. (2011). A new glacier inventory for the European Alps from Landsat TM scenes of 2003: Challenges and results. *Annals of Glaciology*, *52*(59), 144–152. https://doi.org/10.3189/172756411799096295

Paul, F. (2004). Rapid disintegration of Alpine glaciers observed with satellite data. *Geophysical Research Letters*, *31*(21). https://doi.org/10.1029/2004GL020816

Paul, F., Barry, R. G., Cogley, J. G., Frey, H., Haeberli, W., Ohmura, A., Ommnney, C. S. L., Raup, B., Rivera, A., & Zemp, M. (2010). Guidelines for the compilation of glacier inventory data from digital sources. *Annals of Glaciology*, *50*(53), 119–126. https://doi.org/10.3189/172756410790595778

Pfeffer, W. T., Arendt, A. A., Bliss, A., Bolch, T., Cogley, J. G., Gardner, A. S., Hagen, J.-O., Hock, R., Kaser, G., & Kienholz, C. (2014). The Randolph Glacier Inventory: A globally complete inventory of glaciers. *Journal of Glaciology*, *60*(221), 537–552. https://doi.org/10.3189/2014JoG13J176

Radić, V., & Hock, R. (2011). Regionally differentiated contribution of mountain glaciers and ice caps to future sea-level rise. *Nature Geoscience*, *4*(2), 91–94. https://doi.org/10.1038/ngeo1052

Rasmussen, L. A., Conway, H., & Hayes, P. S. (2000). The accumulation regime of Blue Glacier, USA, 1914–96. *Journal of Glaciology*, *46*(153), 326–334. https://doi.org/10.3189/172756500781832846

Rayner, N., Parker, D. E., Horton, E., Folland, C., Alexander, L., Rowell, D., Kent, E., & Kaplan, A. (2003). Global analyses of sea surface temperature, sea ice, and night marine air temperature since the late nineteenth century. *Journal of Geophysical Research: Atmospheres*, *108*(D14), 2156-2202. https://doi.org/10.1029/2002JD002670

Riedel, Jon L., & Larrabee, M. A. (2016). Impact of Recent Glacial Recession on Summer Streamflow in the Skagit River. *Northwest Science*, *90*(1), 5–22. https://doi.org/10.3955/046.090.0103

Riedel, Jon L., Wilson, S., Baccus, W., Larrabee, M., Fudge, T. J., & Fountain, A. (2015). Glacier status and contribution to streamflow in the Olympic Mountains, Washington, USA. *Journal of Glaciology*, *61*(225), 8–16. https://doi.org/10.3189/2015JoG14J138

Riedel, Jon L., & Larrabee, M. A. (2016). Impact of Recent Glacial Recession on Summer Streamflow in the Skagit River. *Northwest Science*, *90*(1), 5–22. https://doi.org/10.3955/046.090.0103

Ropelewski, C. F., & Jones, P. D. (1987). An extension of the Tahiti–Darwin southern oscillation index. *Monthly Weather Review*, *115*(9), 2161–2165.

Schiefer, E., Menounos, B., & Wheate, R. (2007). Recent volume loss of British Columbian glaciers, Canada: Volume loss of BC glaciers. *Geophysical Research Letters*, *34*(16), L16503. https://doi.org/10.1029/2007GL030780

Shea, J. M., & Marshall, S. J. (2007). Atmospheric flow indices, regional climate, and Glacier mass balance in the Canadian Rocky Mountains. *International Journal of Climatology*, *27*(2), 233–247. https://doi.org/10.1002/joc.1398

Spicer, R. (1986). Glaciers in the Olympic Mountains, Washington—Present distribution and recent variations. [M.S.]. University of Washington.

Spicer, R. C. (1989). Recent variations of Blue Glacier, Olympic Mountains, Washington, USA. *Arctic and Alpine Research*, *21*(1), 1–21. https://doi.org/10.2307/1551513

Tangborn, W. V., Fountain, A. G., & Sikonia, W. G. (1990). Effect of area distribution with altitude on glacier mass balance–a comparison of North and South Klawatti Glaciers, Washington State, USA. *Annals of Glaciology*, *14*, 278–282.

Thompson, D. W. J., & Wallace, J. M. (1998). The Arctic oscillation signature in the wintertime geopotential height and temperature fields. *Geophysical Research Letters*, *25*(9), 1297–1300. https://doi.org/10.1029/98GL00950

Thompson, D. W. J., Wallace, J. M., Kennedy, J. J., & Jones, P. D. (2010). An abrupt drop in Northern Hemisphere sea surface temperature around 1970. *Nature*, *467*(7314), 444–447. https://doi.org/10.1038/nature09394

Trenberth, K. E. (1997). The definition of el nino. *Bulletin of the American Meteorological Society*, *78*(12), 2771–2778. https://doi.org/10.1175/1520-0477(1997)078<2771:TDOENO>2.0.CO;2

Trenberth, K. E., & Hurrell, J. W. (1994). Decadal atmosphere-ocean variations in the Pacific. *Climate Dynamics*, *9*(6), 303–319. https://doi.org/10.1007/BF00204745

USDA, 2019. https://www.fsa.usda.gov/programs-and-services/aerial-photography/imagery-programs/naip-imagery/index, accessed March 2017

UW, 2019. http://gis.ess.washington.edu/data/raster/doqs/index.html, data referenced November 2007

UW, (2018). research.jisao.washington.edu/datasets/pdo/

Van Vuuren, D. P., Edmonds, J., Kainuma, M., Riahi, K., Thomson, A., Hibbard, K., Hurtt, G. C., Kram, T., Krey, V., & Lamarque, J.-F. (2011). The representative concentration pathways: An overview. *Climatic Change*, *109*(1–2), 5. https://doi.org/10.1007/s10584-011-0148-z

Wallace, J. M., & Gutzler, D. S. (1981). Teleconnections in the Geopotential Height Field during the Northern Hemisphere Winter. *Monthly Weather Review*, *109*(4), 784–812. https://doi.org/10.1175/1520-0493(1981)109<0784:TITGHF>2.0.CO;2

Walters, R. A., & Meier, M. F. (1989). Variability of Glacier Mass Balances in Western North America. In *Aspects of Climate Variability in the Pacific and the Western Americas* (pp. 365–374). American Geophysical Union. http://dx.doi.org/10.1029/GM055p0365

WGMS, 2019, https://wgms.ch/faqs/ data referenced, February 2019.

Wood, R. L. (1976). *Men, mules, and mountains: Lieutenant O'Neil's Olympic expeditions*. Mountaineers Books.

Zhang, X., Wang, J., Zwiers, F. W., & Groisman, P. Y. (2010). The influence of large-scale climate variability on winter maximum daily precipitation over North America. Journal of Climate, 23(11), 2902–2915. https://doi.org/10.1175/2010JCLI3249.1

Appendix

Uncertainty Assessment of the interpretation uncertainty evolved over time. For the 1990 imagery we followed Spicer (1986) whereby it was visually ranked into three categories: 1) excellent – minimal snow/rock cover or shadows, ±2.5%; 2) good - moderate cover or shadows, ±7.5%; and 3) poor - extensive cover or shadow ±20%. For the 2009 inventory, each glacier was outlined twice. The first outline included only clean and debris-covered ice as indicated by crevasses. The second outline included exposed ice, debris, and seasonal snow. The interpretation uncertainty is one-half of the difference between the two areas outlined. Although more precise, results did not vary significantly from a broader calibrated assessment we applied to the 2015 inventory. The glaciers were visually grouped into two categories low and high uncertainty. A subset of 37 (low) and 34 (high) glaciers were than outlined using the min/max method. The difference between the minimum and maximum outline was then normalized to the glacier area and an average was calculated for the two groups. The low category had a ± 4% uncertainty, and the high had ± 16% uncertainty.

Table A1. *Comparison of the topographic characteristics for the most and least changed glaciers from the quartile analysis. Elev is elevation, Asp – aspect, Win – winter, Sum – summer, Ann – annual, Temp – air temperature, Precip – precipitation Long – longitude, Lat – latitude, Frac Chg – fractional area change From: Olympic-Wilson-ReAnalysis/Quartile*

	Largest fractional change	Standard deviation	Least fractional change	Standard deviation	Upper minus lower
Mean Slope	21	5	23	6	-3
Mean Elev	1612	149	1764	124	-152
Max Elev	1672	159	1923	183	-250
Min Elev	1566	158	1598	181	-32
Mean Asp	207	157	211	144	-5
Win Precip	2697	1019	2655	1035	42
Win Temp	-1.7	0.9	-2.4	0.9	0.7
Sum Temp	9.3	0.8	8.7	0.8	0.6
Ann. Precip	3730	1429	3622	1482	108
Ann Temp	2.8	0.8	2.2	0.8	1
Mean Long	-123.6	0.2	-123	0.2	-0.1
Mean Lat	47.8	0.1	48	0.1	0.0
Mean Area	0.06	0.09	0.56	1.19	-0.50
Mean Frac Chg	-0.98	0.03	-0.37	0.12	-0.61
Number	54		55		

Table A2. *The area (km^2) of Blue Glacier used for the mass balance model. The area for the years 1915 – 1982 were from Spicer (1989). The area for 1990 – 2015 came from our analysis. The area is that of the trunk glacier and does not include the 'snow dome' which did not change in area over the time observed.*

Year	Area
1815	5.98
1900	5.61
1906	5.61
1912	5.61
1913	5.61
1915	5.61
1919	5.61
1924	5.57
1933	5.38
1939	5.31
1952	5.21
1957	5.23
1964	5.22
1965	5.22
1966	5.23
1967	5.23
1968	5.23
1970	5.24
1976	5.30
1977	5.30
1978	5.30
1979	5.31
1981	5.31
1982	5.30
1990	5.08
2009	4.71
2015	4.47

Table A3. *Correlations between monthly values modeled glacier mass balance, air temperature, and precipitation, and various climate indices over the period 1900-2014, all smoothed by a 1-year running mean. The bold indicates the highest correlations between the indexes and glacier-local measurements. The abbreviations are, ppt –precipitation (mm), temp – average air temperature, MB – mass balance, Nino 3.4 – sea surface temperature anomaly in the 3.4 region*

of the Pacific Ocean, PDO – Pacific decadal oscillation, PNA – Pacific North America, SOI – Southern oscillation index, NP – North Pacific. See text for citations and data sources.

	ppt	*temp*	*MB*	*Nino 3.4*	*PDO*	*PNA*	*SOI*	*NP*	*NAO*	*Sunspots*
ppt	1.00									
temp	-0.12	1.00								
MB	0.52	-0.74	1.00							
Nino 3.4	-0.13	0.52	-0.43	1.00						
PDO	-0.19	**0.53**	**-0.52**	0.55	1.00					
PNA	-0.11	**0.64**	**-0.59**	0.53	0.66	1.00				
SOI	0.15	-0.47	0.40	-0.83	-0.54	-0.47	1.00			
NP	0.15	**-0.58**	**0.56**	-0.45	-0.58	-0.71	0.48	1.00		
NAO	0.08	0.05	0.05	0.04	0.01	-0.15	-0.11	0.18	1.00	
Sunspots	-0.04	0.09	-0.11	0.03	-0.06	-0.08	0.01	-0.05	0.15	1.00

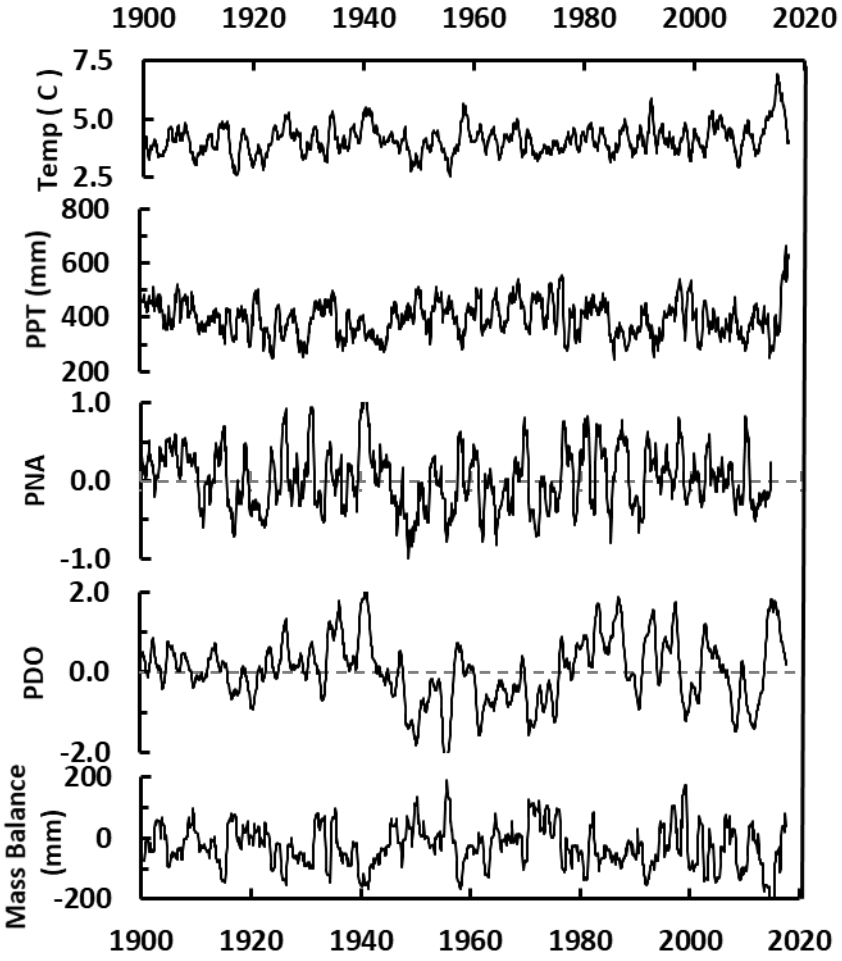

Figure A1. Smoothed time series (1 year) of monthly local air temperature, precipitation, two climate idiocies (PNA – Pacific North America; PDO – Pacific Decadal Oscillation) and modeled glacier mass balance.